

Identification of Novel Binding Interactions in the Development of Potent, Selective 2-Naphthamidine Inhibitors of Urokinase. Synthesis, Structural Analysis, and SAR of *N*-Phenyl Amide 6-Substitution

Michael D. Wendt,^{*,†} Todd W. Rockway,[†] Andrew Geyer,[†] William McClellan,[†] Moshe Weitzberg,[†] Xumiao Zhao,[†] Robert Mantei,[†] Vicki L. Nienaber,[‡] Kent Stewart,[‡] Vered Klinghofer,[†] and Vincent L. Giranda[†]

Cancer Research and Structural Biology, Global Pharmaceutical R & D, Abbott Laboratories, 100 Abbott Park Road, Abbott Park, Illinois 60064-6101

Received January 7, 2003

The preparation and assessment of biological activity of 6-substituted 2-naphthamidine inhibitors of the serine protease urokinase plasminogen activator (uPA, or urokinase) is described. 2-Naphthamidine was chosen as a starting point based on synthetic considerations and on modeling of substituent vectors. Phenyl amides at the 6-position were found to improve binding; replacement of the amide with other two-atom linkers proved ineffective. The phenyl group itself is situated near the S1' subsite; substitutions off of the phenyl group accessed S1' and other distant binding regions. Three new points of interaction were defined and explored through ring substitution. A solvent-exposed salt bridge with the Asp60A carboxylate was formed using a 4-alkylamino group, improving affinity to $K_i = 40$ nM. Inhibitors also accessed two hydrophobic regions. One interaction is characterized by a tight hydrophobic fit made with a small dimple largely defined by His57 and His99; a weaker, less specific interaction involves alkyl groups reaching into the broad prime-side protein binding region near Val41 and the Cys42-Cys58 disulfide, displacing water molecules and leading to small gains in activity. Many inhibitors accessed two of these three regions. Affinities range as low as $K_i = 6$ nM, and many compounds had $K_i < 100$ nM, while moderate to excellent selectivity was gained versus four of five members of a panel of relevant serine proteases. Also, some selectivity against trypsin was generated via the interaction with Asp60A. X-ray structures of many of these compounds were used to inform our inhibitor design and to increase our understanding of key interactions. In combination with our exploration of 8-substitution patterns, we have identified a number of novel binding interactions for uPA inhibitors.

Introduction

Urokinase-type plasminogen activator (uPA), or urokinase, is a trypsin-family serine protease that converts plasminogen into the active enzyme plasmin, a wide-spectrum protease that digests various components of the extracellular matrix and also activates proenzymes of matrix metalloproteinases. Urokinase is secreted by tumor cells or adjacent stroma and exists either as the free enzyme or bound to its cell-surface receptor, uPAR. Binding to uPAR significantly increases the rate of cell-surface-associated plasminogen activation by urokinase and can serve to spatially focus its activity. The uPA/uPAR complex plays a role in many normal physiological events, such as wound healing, but is also involved in tissue remodeling processes of many diseases, including arthritis,¹ atherosclerosis,² vascular restenosis,³ and cancer. In particular, urokinase is implicated in many tumor-associated processes, including extracellular matrix degradation, invasion, angiogenesis, and metastasis.^{4,5}

Elevated levels of urokinase are common to many cancer cell lines and are correlated with enhanced

invasiveness and metastasis and poor prognosis.⁵ Transgenic animals deficient in urokinase have shown slower progression of induced tumors.⁶ The same has been shown for plasminogen-deficient animals.⁷ Moreover, small-molecule urokinase inhibitors have been shown to slow primary tumor growth and metastasis.^{8–12}

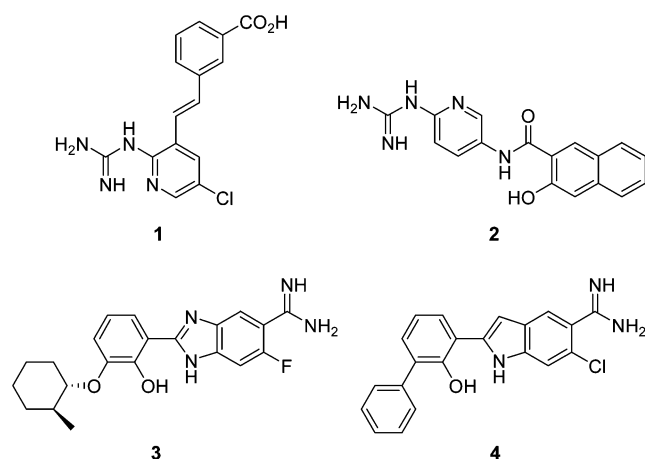
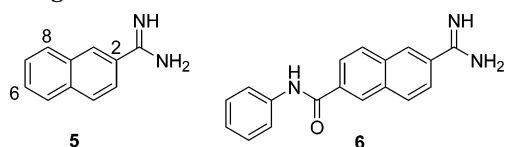
Small-molecule urokinase inhibitors have thus far featured amidines or guanidines, positively charged arginine-mimetic groups that form a salt bridge with the Asp189 carboxylate in the S1 pocket of the active site of urokinase and other trypsin-like serine proteases. Typical early inhibitors were aryl amidines or guanidines with minimal substitution.^{13–18} These compounds normally exhibited single- or double-digit micromolar activities. Additionally, while the aryl guanidines as a group showed some selectivity for urokinase, and to a lesser extent trypsin, versus a number of other physiologically relevant trypsin-like proteases,^{15a} the class of early inhibitors, largely confined to the S1 subsite, lack sufficient potency and selectivity to be therapeutically useful. Chart 1 shows some examples (**1–4**) of recently reported urokinase inhibitors that are more structurally elaborate and generally show increased potency and selectivity.^{19–24}

Rationale. Our efforts began with investigation of a number of bicyclic aromatic amidine cores. On the basis of information accumulated from substituent SAR on

* To whom correspondence should be addressed: Abbott Laboratories, D-4N6, AP10/3, 100 Abbott Park Road, Abbott Park, IL 60064. Tel: (847) 937-9305. Fax: (847) 935-5165. E-mail: mike.d.wendt@abbott.com.

[†] Cancer Research.

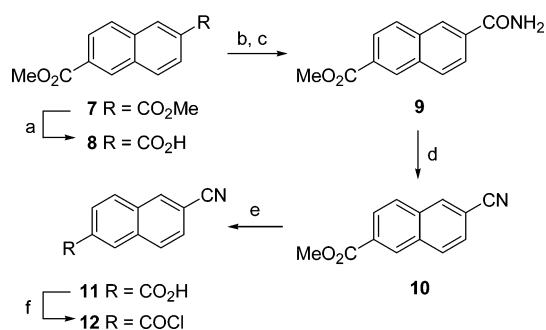
[‡] Structural Biology.

Chart 1. Amidine and Guanidine Inhibitors of UPA**Chart 2.** Naphthamide UPA Inhibitors with Numbering Scheme

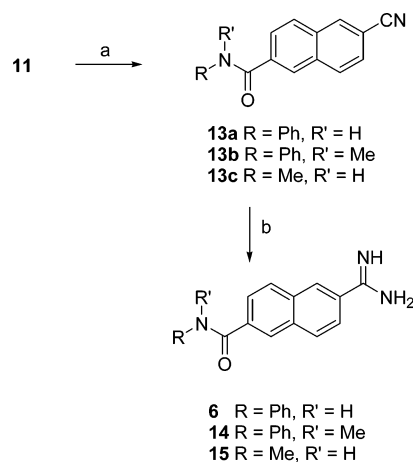
these series and on structure-based determinations of the viability of further substitution, we decided to focus on 2-naphthamide **5**¹³ as the scaffold for further work. **5** itself has good affinity for urokinase ($K_i = 5.9 \mu\text{M}$) relative to other aromatic amidines, and exhibits some selectivity on its own against tPA and plasmin. Selected aspects of our work with derivatives of **5**, detailing X-ray structural studies on 8-substitution²⁵ and species specificity,²⁶ have already been reported.

Both modeling and testing of several variously substituted naphthamides led us to conclude that the 6, 7, and 8 positions would tolerate substitution. Our approach was to initially investigate each substituent vector separately, assuming that a later combination of our best substituents at each site would likely give approximately additive affinities. We felt, and subsequent crystallographic data confirmed, that the relatively tight fit of the 2-naphthamide core in the S1 subsite of urokinase would help ensure the validity of such an approach.²⁵ Modeling led us to expect that substituents at position 7 would project into solvent, and an initial determination of the lack of any effect on potency of several substituents led us to quickly abandon work at that site. We then concentrated our efforts on exploring the effects of substitution at the 6 and 8 positions. Here we report on the synthesis and development of 6-substituted 2-naphthamide urokinase inhibitors, including structure–activity relationships of the phenyl amide **6**. In the future we will report further on 8-substitution and on fully elaborated, disubstituted 2-naphthamides.

Chemistry. Our general synthetic approach rested on several factors. Given that the polarity and basicity of the amidine group make it undesirable to carry through a number of synthetic steps, and that there exist many methods of synthesizing amidines from nitriles, we targeted the cyano acid **11** and acid chloride **12** as cores from which we could generate a large number of amide-containing compounds. It was thus

Scheme 1

Reagents and conditions: (a) KOH, dioxane, Δ ; (b) SOCl_2 , toluene, Δ ; (c) NH_3 , CH_2Cl_2 ; (d) TFAA, pyridine, dioxane; (e) LiOH, THF, H_2O ; (f) $(\text{COCl})_2$, toluene, Δ .

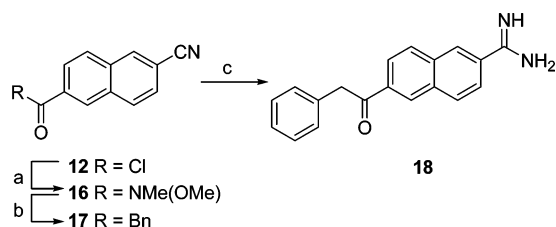
Scheme 2

Reagents and conditions: (a) amine, HATU, $i\text{Pr}_2\text{NEt}$, DMF; (b) $\text{LiN}(\text{TMS})_2$, THF; then aq. HCl.

important to find a synthesis of **11/12** amenable to large-scale work and requiring no chromatography. Scheme 1 shows this synthesis. We were able to start with the inexpensive diester **7**; monosaponification gave the acid **8**, which was converted via the acid chloride to the amide **9** in 89% yield. Dehydration to the nitrile **10** could be easily performed in a number of ways; the cleanest used TFAA/pyridine and gave the nitrile in 94% yield.²⁷ Another saponification quantitatively gave the cyano acid **11**, which was easily carried on to pure acid chloride **12** by refluxing in toluene with oxalyl chloride and condensing from toluene. It became convenient to produce and store **12** in large quantity.

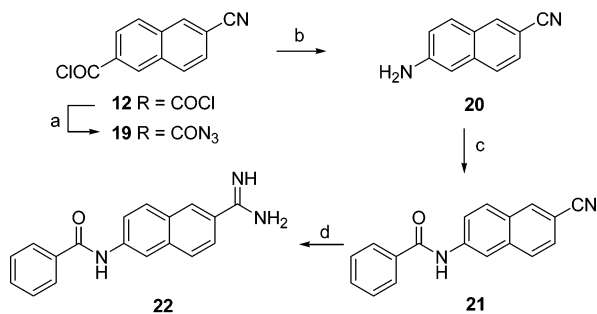
Scheme 2 shows the syntheses of the parent amide **6**, its *N*-methyl derivative **14**, and the *N*-methylamide **15**. Early synthetic efforts did not employ **12**; instead, the acid **11** was used to couple to amines. Anilines were found to be unreactive toward **11** with most coupling agents; however, HATU in DMF gave sufficient yields of amides. **13a–c** were then transformed to amidines **6**, **14** and **15** via nucleophilic attack on the nitriles by $\text{LiN}(\text{TMS})_2$, followed by hydrolysis of the silyl groups with aqueous HCl.²⁸ This method of amidine synthesis proved over time to be operationally simplest and compatible with most functional groups. Normally the nitriles were cleanly and completely transformed to amidines, and groups with active hydrogens in the substrate, such as the amide NH, usually necessitated

Scheme 3



Reagents and conditions: (a) MeNHOMe·HCl, CH₂Cl₂; (b) BnMgCl, THF; (c) HCl, MeOH; then NH₄OAc, MeOH.

Scheme 4



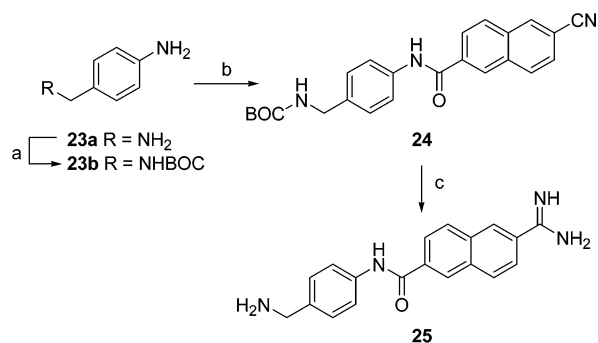
Reagents and conditions: (a) NaN₃, acetone, H₂O; (b) H₂SO₄; (c) PhCOCl, dioxane, K₂CO₃; (d) H₂S, pyridine, Et₃N; then MeI; then NH₃.

only the use of a larger excess of LiN(TMS)₂. Yields varied significantly; while HPLC purification usually produced high (70–90%) yields, occasional transformation to different salt forms and recrystallization, after or in place of HPLC purification, could result in final yields of between 15 and 90%.

We were able to use **12** in the syntheses of the ketone and reverse amide analogues of **6**. Scheme 3 shows the synthesis of the benzyl ketone **18**. Formation of the Weinreb amide **16** from **12** is followed by benzyl Grignard addition to give the ketone **17** in 28% yield. Due to the presence of the enolizable ketone functionality, the Pinner reaction²⁹ was used to make **18**. For the reverse amide synthesis, shown in Scheme 4, sodium azide was added to the acid chloride **12** to give **19**, which was decomposed to the amine **20** by treatment with H₂SO₄. The amine was coupled to benzoyl chloride, and the resulting amide **21** was transformed to the amidine **22** via the thioamide and thioimidate ester, using the method of Bredereck et al.³⁰

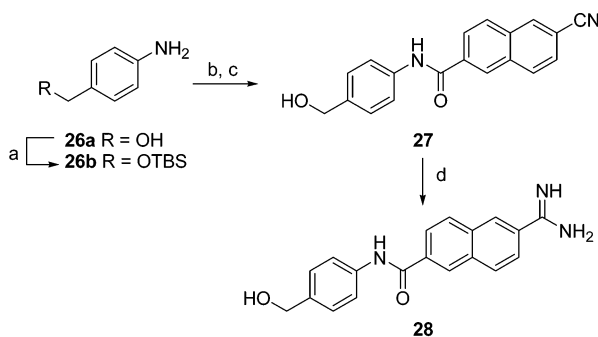
With amide targets formally reduced to aniline syntheses, 4-(aminomethyl)aniline **23a** was protected with di-*tert*-butyl dicarbonate (Scheme 5), giving **23b**, before coupling to the acid **11** with HATU to give amide **24**. Amidination to **25** was achieved using the LiN(TMS)₂ protocol, with BOC deprotection taking place during acidic silyl group hydrolysis. Similarly for the corresponding 4-hydroxymethyl compound (Scheme 6), the alcohol **26a** was protected with TBSCl, and the aniline **26b** coupled with **11** using HATU. The crude product was deprotected to the alcohol **27** with TBAF, and the amidine **28** was produced via LiN(TMS)₂. The 4-ethyl compound, precursor **29a**, was taken on to the amide via **11** as before, but for amidoaniline **29b** the acid chloride **12** was used (Scheme 7). Products **30a** and **30b** were transformed into amidines **31a** and **31b** via the thioamide and Pinner protocols, respectively.

Scheme 5



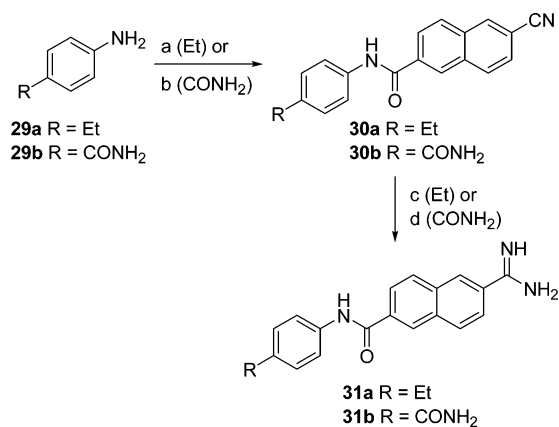
Reagents and conditions: (a) (BOC)₂O, THF, H₂O; (b) **11**, HATU, iPr₂NEt, DMF; (c) LiN(TMS)₂, THF; then aq. HCl.

Scheme 6



Reagents and conditions: (a) TBSCl, imidazole, DMF; (b) **11**, HATU, iPr₂NEt, DMF; (c) TBAF, THF; (d) HCl, MeOH; then NH₄OAc, MeOH.

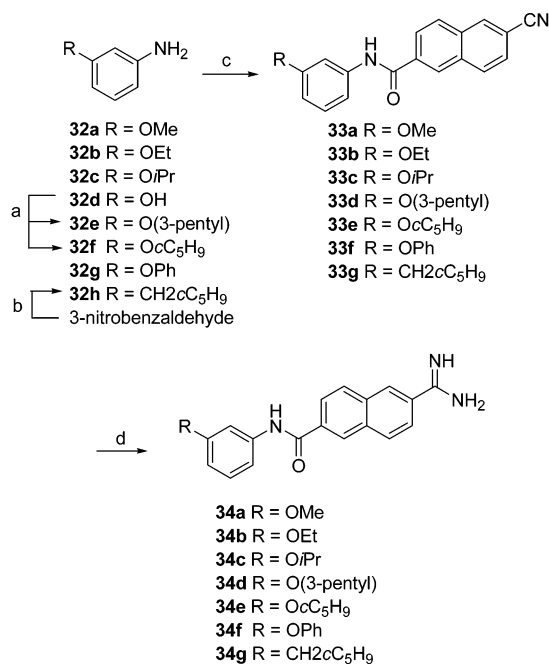
Scheme 7



Reagents and conditions: (a) **11**, HATU, iPr₂NEt, DMF; (b) **12**, Et₃N, DMAP; (c) H₂S, pyr., Et₃N; then MeI; then NH₃; (d) HCl, MeOH; then NH₄OAc, MeOH.

The 3-alkoxy series syntheses are shown in Scheme 8. The alkoxyanilines **32e** and **32f** were made under standard Mitsunobu conditions in excellent yields. The cyclopentylmethyl analogue **32i** was made in 81% yield from aldehyde **32h** via Wittig reaction with cyclopentyltriphenylphosphonium bromide, followed by immediate one-pot reduction of the nitro and olefin groups. The bis-ether syntheses (Scheme 9) began with 3,5-dimethoxyaniline, **35a**, and its monodemethylation with NaSm₂.³¹ Yields for this procedure were typically in the 30–60% range; however, single products were obtained and Lewis acid reagents had proved unsuccessful.

Scheme 8



Reagents and conditions: (a) ROH, PPh₃, DEAD, THF; (b) C₅H₉PPh₃Br, BuLi, THF; then H₂, 10% Pd/C, MeOH; (c) **12**, Et₃N, DMAP; (d) LiN(TMS)₂, THF; then aq. HCl.

Mitsunobu alkylation with 2-propanol then gave **35c** from **35b**. Treatment of **35c**, again with NaSMe, selectively provided the phenol **35d**, which similarly was made to undergo Mitsunobu alkylation with 2-propanol or cyclopentanol to give **35e** and **35f** in 83% and 87% yields, respectively. All appropriately substituted anilines **32a–c,e–h** and **35a,e,f** were coupled to **12** to give amides **33a–g** and **36a–c** in 60–90% yields, which were in turn subjected to the LiN(TMS)₂ protocol to give amidines **34a–g** and **37a–c**.

Synthesis of the 7-aminodihydroisoquinoline derivatives (Scheme 10) began with the synthesis of **39c** and the known **39a,b**,³² via acylation of phenethylamine **38a** followed by cyclodehydration with FeCl₃.³³ Nitration with KNO₃ in H₂SO₄ to give **40a–c** was followed by selective reduction of the nitro groups using Raney nickel to give the iminoanilines **41a–c**. The corresponding tetrahydroisoquinolines were obtained by reducing **41a–c** to amines **44a–c** with sodium borohydride, followed by BOC protection. The syntheses were again finished by coupling of the imines **41a–c** and protected amines **45a–c** and subsequent formation of amidines from **42a–c** and **46a–c** with LiN(TMS)₂, giving **43a–c** and **47a–c**, with BOC deprotection again taking place upon desilylation.

The related 6-aminotetrahydroisoquinolines **56a,b** were made by modifying a route reported by Quallich et al.³⁴ (Scheme 11). The known **48**³⁴ was alkylated and esterified to afford **49**. Saponification and decarboxylation led to **50**, followed by borane reduction to give the diol **51a**, which, along with the known **51b**,³⁴ was bis-mesylated and displaced *in situ* by allylamine to afford the tetrahydroisoquinolines **52a,b**. Reduction of the nitro groups to amines **53a,b** was accomplished with viologen,³⁵ and the amides **54a,b** were formed from the acid chloride **12** as above in high yields. After LiN(TMS)₂ amidine formation, deallylation of amines **55a,b**

to products **56a,b** was accomplished cleanly using Pd⁰ and thiosalicylic acid.³⁶

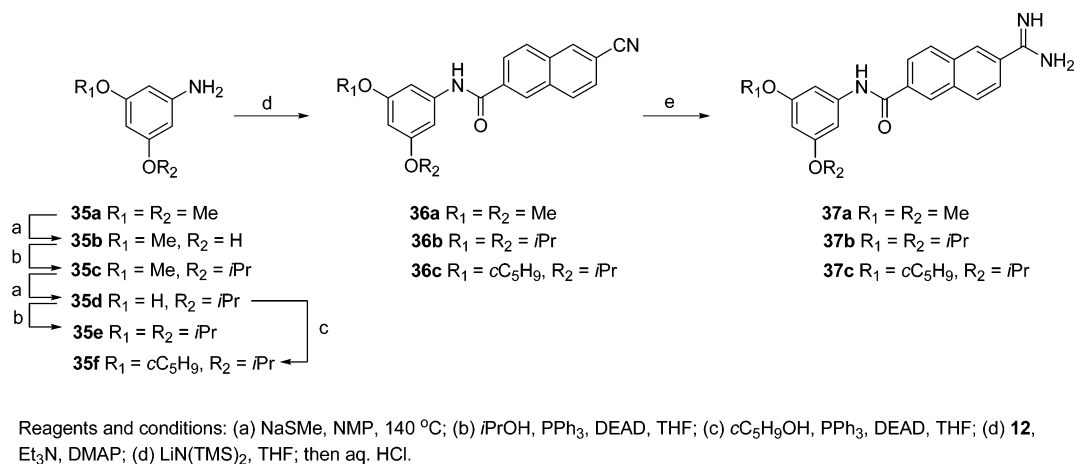
Results and Discussion

Access to Secondary Binding Sites. Trypsin-like serine protease inhibitor design has commonly targeted the S2 and S4 and occasionally S3 subsites, as illustrated by work on enzymes such as factor Xa or thrombin.³⁷ In addition to the expected improvements in activity, interactions with these sites often lead to an increase in selectivity against other trypsin-like serine proteases. Urokinase, however, possesses a two-amino acid insertion of Thr97A and Leu97B (chymotrypsin numbering system), which partially eclipses the opening of, and drastically reduces the size of, S4.³⁸ The S2 subsite is also small, due to the relatively large His99; similarly for tPA and factor Xa, Tyr99 makes S2 a relatively less important subsite. An excellent illustration of this effect is provided by looking at natural substrates of uPA, which uniformly have small hydrophobic residues at P2, along with hydrophobic residues of various sizes at P1'.³⁸ P3 residues project their side chains into solvent or pack against the protein surface; consequently, the exposed S3 allows a wide variety of hydrophilic residues. The narrow and partially occluded S4 subsite permits a range of hydrophobic and polar P4 residues, with little size restriction seen among natural substrates. Thus, the reduced size of S2 and S4 in urokinase relative to other trypsin-like proteases reduces their likely value as secondary targets for a synthetic inhibitor, and it may be equally fruitful to explore less traditional subsites.³⁹

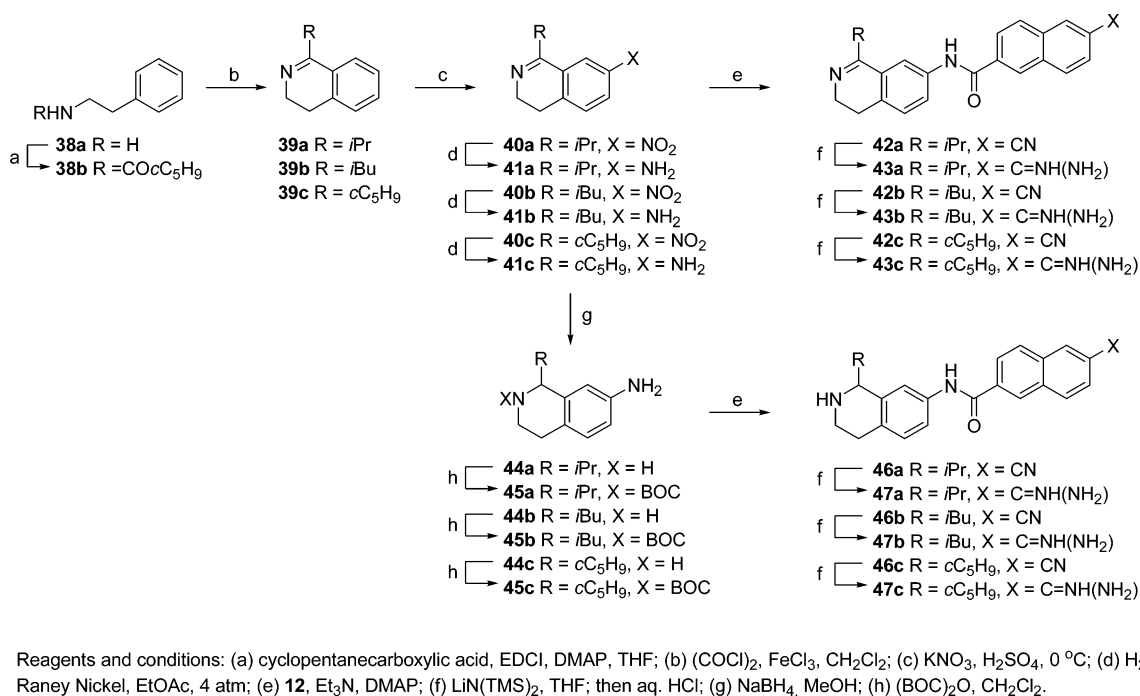
The direct vector off of the 6 position of 2-naphthamidine extends past the S2 subsite. For S2 and S4 to be reachable, a naphthamidine-based inhibitor would require a linking group that would "double back" toward the S4 subsite. The crystal structure of urokinase complexed with a Glu-Gly-Arg-chloromethyl ketone tripeptide inhibitor, mimicking a natural substrate, has shown how this doubling back can be accomplished.³⁸ Again, though, the relative narrowness of S4 requires a level of precision in the geometry of a non-peptide inhibitor that may prove difficult to build onto a typical aromatic amidine or guanidine scaffold. Early efforts of ours sought to do just this, but we were unable to access the S4 pocket, and none of a large series of inhibitors designed for this displayed a gain in activity. Still, the 6 position offers access to other regions of the urokinase surface, including the S1' site, which leads directly to the broad, shallow prime-side protein binding region that other programs have had some success in exploring,^{21,23a,24} and still other, non-peptide binding distant sites. We were able to identify structures that gave rise to interactions with S1' and some of these other, more distant regions of the urokinase surface.

Structure–Activity Relationships and Structural Analysis. Our early inhibitors were built with the intent to explore the precise nature of vectors pointing away from the naphthyl core. Among these compounds, the phenyl amide **6** showed a 10-fold improvement in potency against urokinase compared to the parent **5** (Table 1). Many of our inhibitors were evaluated for selectivity against a panel of physiologically important trypsin-like serine proteases involved

Scheme 9



Scheme 10

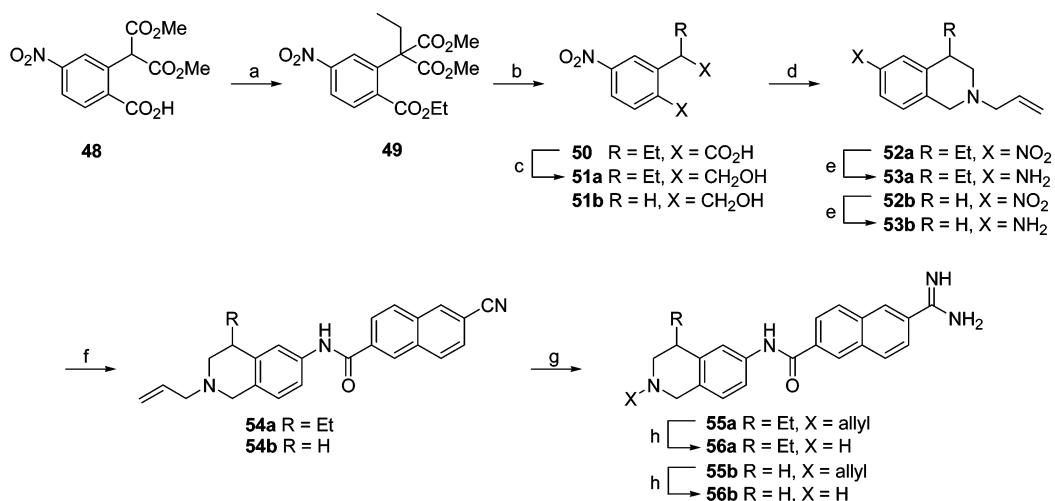


in coagulation and proteolysis. For **6**, selectivities were substantially the same as for **5**, changing by only as much as 3-fold in either direction.

As noted above, **5** itself possesses a modicum of selectivity toward tPA and plasmin. Selectivity patterns for various S1-only aromatic amidines have been discussed partly in terms of the identity of residue 190.^{23b,40} Aromatic amidines tend to bind with a small preference for Ser190-containing proteases, including uPA, trypsin, and plasmin, compared to Ala190 proteases such as tPA, thrombin, and kallikrein. A glance at Table 1 indicates that, for **5**, other factors must play a role, especially for plasmin; however, the high homologies of S1-forming residues and resulting structural similarities of the proteases in question make elucidation of other factors challenging at best.^{40a} We do note that the overall selectivity pattern of **5** roughly parallels that of other aromatic amidines, benzo[*b*]thiophene-2-carboxamidines and even to some extent benzamidines,^{40a} though **5** does show a small improvement in selectivity with respect to tPA.

Figures 1 and 2a show aspects of the X-ray structure of **6** bound to urokinase. The **6**-uPA complex structure shows the naphthyl group anchored in the active site by a typical salt bridge between the amidine and Asp189. The interatomic distances are typical, at 2.9 and 3.0 Å, and show little variation between compounds in this series. In general, our various inhibitor-uPA structures exhibit very small differences in rotation about the long axis of the naphthyl groups within S1 and almost no variation with respect to movement toward or away from Asp189. The amide is situated above the active site Ser195, with the phenyl group extending beyond S2 toward the protein binding region. Key to the amide conformation is its involvement in a hydrogen-bonding network. Figure 1 highlights aspects of this network. The amide NH is involved in a water-mediated hydrogen bond to Ser214 O_γ. The bridging water molecule is well-ordered, with a temperature (*B*) factor of 7.5, and is similarly located in all of our amide inhibitor-uPA complex X-ray structures. On the other side, the amide carbonyl seems to interact with Gln192

Scheme 11



Reagents and conditions: (a) EtI, K₂CO₃, acetone, Δ; (b) aq. NaOH, EtOH, Δ; (c) BH₃, THF; (d) MsCl, Et₃N, THF; then allylamine; (e) Viologen, K₂CO₃, Na₂S₂O₄, CH₂Cl₂, H₂O; (f) **12**, Et₃N, DMAP; (g) LiN(TMS)₂, THF; then aq. HCl; (h) Pd(dba)₂, dppb, thiosalicylic acid, THF, DMF.

Table 1. Amide Linker Binding and Effect of Changes to the Nature of the Linking Group

R	R	K _i (μM) ^a					
		uPA	kallikrein	tPA	trypsin	plasmin	thrombin
5	H	5.91	22.5	>100	7.78	51.3	-
6		0.631 ± 0.086	2.50 ± 1.14(9)	31.8 ± 17.8(9)	0.325 ± 0.175(8)	1.95 ± 0.58(9)	5.64 ± 2.16(9)
14		15.5 ± 0.4	-	-	-	-	-
15		8.70	-	-	-	-	-
18		7.98	-	-	-	-	-
21		1.90	8.00 ± 2.98	>100	2.61 ± 0.06	5.56 ± 1.65	17.6 ± 3.40

^a ± standard deviation (number of determinations if more than two). All determinations are triplicate values.

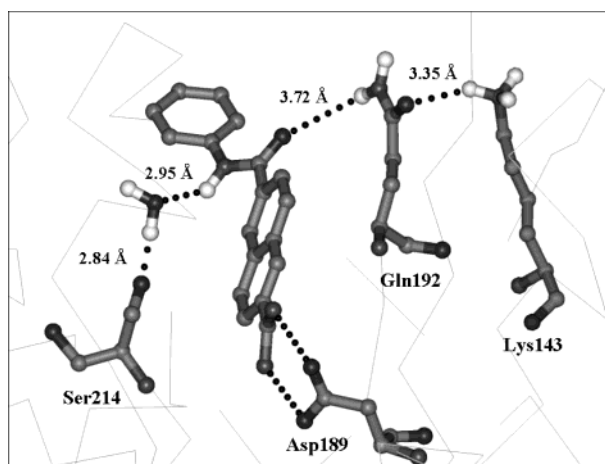


Figure 1. View of the hydrogen-bonding network in the **6**-uPA complex. Hydrogen bonds are drawn to H atoms, while labeled distances are heavy atom to heavy atom. The naphthyl-amide dihedral angle is 29° and the amide-phenyl dihedral angle is 31°.

Nε2, which is in turn hydrogen-bonded through its amide carbonyl to Lys143 Nζ. All aspects of this hydrogen-bonding network were found in each of our

inhibitor-uPA X-ray structures, though hydrogen-bond distances and angles varied, in some cases considerably. For many of the interactions seen in the **6**-uPA complex, geometries and distances are not optimal; first, the **6**-Gln192 Nε2 hydrogen-bond angle is closer to orthogonal than linear, and the distance of 3.7 Å is much longer than the normal hydrogen-bond distance of 2.8–3.2 Å. Interestingly, the Gln192 Nε2-Lys143 Nζ hydrogen bond is also longer than is typical (3.4 Å), and it appears that both of these distances, and the geometry of the former interaction, could be significantly improved with simple rotation and possibly translational movement of Gln192. At any rate, in most of the amide-uPA complex X-ray structures the amide carbonyl-Gln192 Nε2 hydrogen bond assumes a much more normal distance. The amide NH-Ser214 Oγ water-mediated hydrogen bond is more typical, with distances of 3.0 and 2.8 Å from **6** to the water molecule to Ser214 Oγ. Here again, the amide NH-H₂O angle, calculated to be 141°, is not ideal but is within the range of normally acceptable values.

The amide conformation is also partly determined by other features evident in the complexed structure. The amide has an energetic preference to remain in a near-

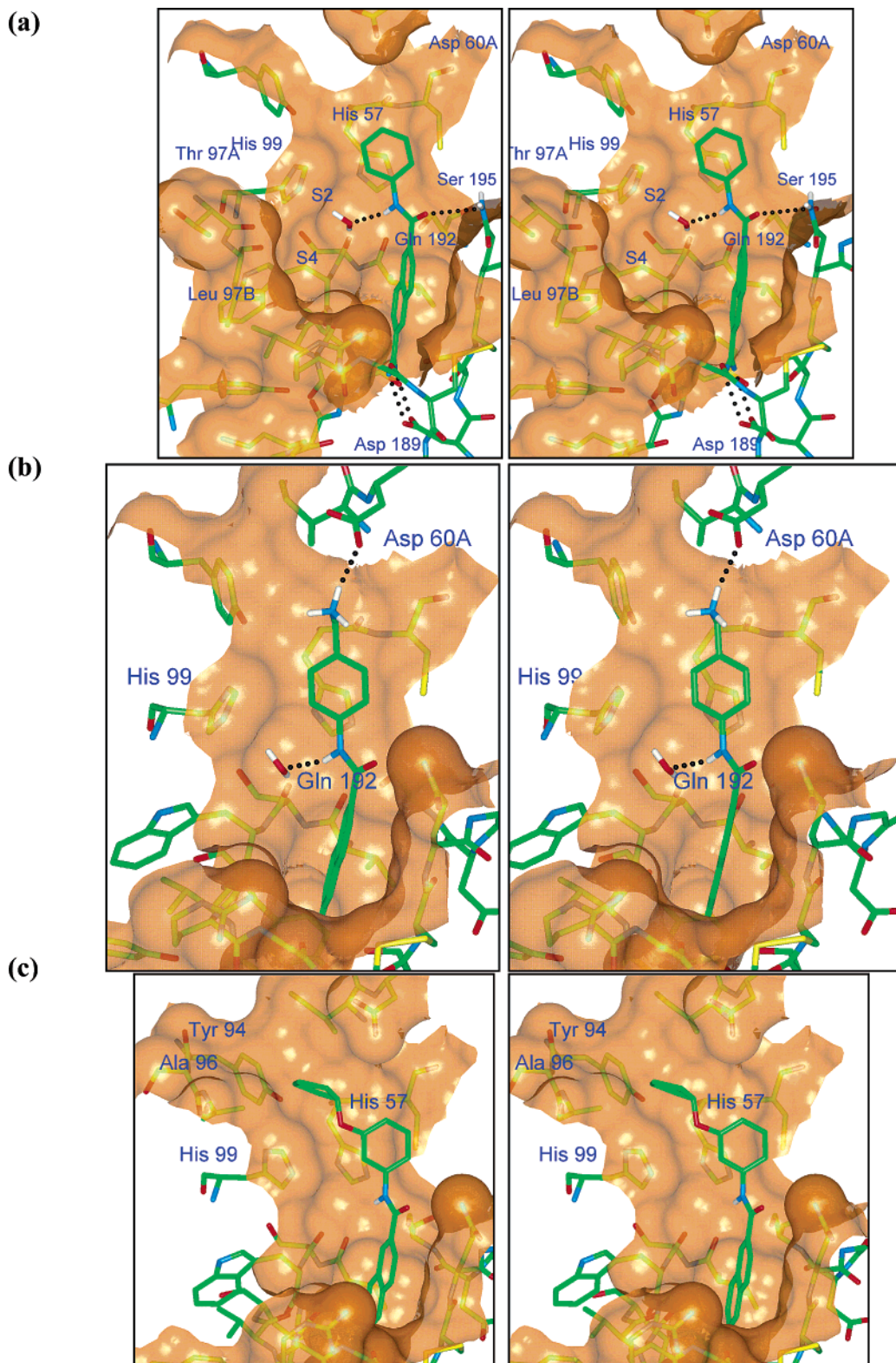


Figure 2. Stereoviews of parent and monosubstituted amides in crystal structures of uPA complexes, with Connolly surfaces. (a) **6** bound to uPA. Residues within 6 Å of **6** are shown along with their solvent-accessible Connolly surfaces (orange). Hydrogen bonds are shown by dotted lines. The water involved in a hydrogen bond with Ser214 and **6** is shown, above Ser214 O γ and partially occluded by the protein surface. The surface near Gln192 and Asp189 has been removed to permit viewing of the hydrogen-bonding interactions with inhibitor. Approximate locations of the S2 and S4 subsites are indicated, showing the truncation of the subsites by the Thr97A-Leu97B insertion. The phenyl group sits atop the narrow valley defined by the His57 side chain. The Cys58 half of the Cys58-Cys42 disulfide, at the bottom of the prime-side protein binding cleft, is also shown. The active site Ser195 is just visible, below the amide. (b) **25** bound to uPA. The surface near Asp60A is removed to permit viewing of the interaction with the protonated amine of **25**. The distance from the amino group of **25** to Asp60A O δ 2 could be reduced by rotation of the C–N bond, but the amine is rotated toward solvent, maximizing interaction with solvent while still maintaining a good distance (3.2 Å) from Asp60A O δ 2. The hydrogen bond to Gln192 N ϵ 2 is shorter than for **6**. (c) **34e** bound to uPA, with the view turned slightly and the surface extended beyond that in Figure 3a to illustrate the small hydrophobic dimple comprised by His 99, Ala96, Tyr94, and His57. The cyclopentyl group fits well edge-on into the dimple between His99 and Asp60A.

coplanar arrangement with the naphthyl and phenyl groups, but it is required to adopt an out-of-plane conformation in order to form the hydrogen bonds just discussed and to situate the phenyl group in an orientation allowing for interaction with the protein surface. The out-of-plane amide–naphthyl angle of 29° for the **6**–uPA complex, as well as the amide–phenyl out-of-plane angle of 31°, are representative within a few degrees of all our amide–uPA crystal structures. These angles allow for some interaction of the contiguous π -systems, while more importantly situating the phenyl group near the urokinase surface and creating good hydrophobic contact with a relatively flat region of the protein where there is little in the way of a well-defined binding pocket (Figure 2a). This portion of the surface of urokinase is largely defined by the imidazole side chain of the highly conserved active site residue His57. The flat, near-parallel nature of the two rings in the crystal structure allows for good surface contact and possibly generates a π -stacking interaction. The surface beyond the phenyl group in the direction of the conserved Cys58–Cys42 disulfide bond then drops off slightly, near the S1' binding site.

Given the water-mediated and solvent-exposed nature of the hydrogen bonds with Ser214 and Gln192, respectively, and the less than ideal geometries of those interactions, we surmise that the hydrogen-bonding network contributes little to the 10-fold gain in affinity for **6** relative to **5**, but it does importantly allow the hydrophobic contact between the phenyl group and the His57-defined protein surface, which probably is the main driver of the affinity increase. In support of this is the measured affinity of the *N*-methyl amide **15**, which lacks only the hydrophobic interaction and is roughly equipotent with **5** (Table 1). Other related compounds probed different aspects of the amide linker structure. The *N*-methylation of **6** led to **14**, which was less active than 2-naphthamide. The presence of the methyl group in **14** not only eliminates the water-mediated hydrogen-bonding interaction with Ser214 but also produces a steric clash with the naphthyl 5-H, necessitating an increase in the out-of-plane angle, and a further reduction in any favorable interaction with Gln192. Replacement of the NH with a methylene (**18**) also reduced activity. Here, again, there is no possibility of a water-mediated hydrogen bond with Ser214 O γ , and the more rotatable H₂C–CO bond contributes an entropic cost to binding in the most favorable conformation, compared to the rigidity and preferred trans nature of the amide bond.

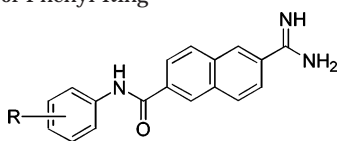
A number of two-atom linkers less closely related to the amide of **6** also failed to increase affinity to uPA. It is likely that less rigid linking groups fail to adequately restrict the possible locations of the phenyl group, ultimately favoring its extension into solvent, while even other rigid linkers such as **14** and **21** lack a precise set of interactions necessary to counter entropic contributions to overall energetics and situate the phenyl group near the protein surface. The reverse amide **21**, which showed improved binding not only to urokinase but all the members of the selectivity panel, was still inferior to **6**. The conformation of **21** bound to urokinase was not determined; however, it probably has the capacity to form a different set of hydrogen bonds with some of

the same residues involved in the binding of **6**. Nevertheless, it is unlikely that **21** is able to situate the phenyl group in a manner similar to **6**. Later amide inhibitors with improved potency over **6** were sometimes made with alternate linking groups, such as the reverse amide, and were always much less active than the corresponding amide.⁴¹ This again demonstrates that only the amide places the phenyl group near the protein surface and His57, and while the improved binding of **6** ultimately derives from the hydrophobic interaction of the phenyl group, the nature of the linking group is crucial.

As noted above, and as the data in Table 1 indicates, selectivities for **6** are roughly similar to those for **5**. That the presence of the phenyl amide has little effect on selectivity is not surprising, as both the His57 and Ser214 are unchanged across the selectivity panel. Moreover, among the members of the panel, the Gln192 of urokinase is only substituted in the case of kallikrein with a lysine, which may also be able to hydrogen bond to the amide carbonyl, and in the case of thrombin with a glutamic acid, which cannot. Thus, the majority of the small selectivity changes on going from **5** to **6** are likely driven by more subtle factors not evident from the primary interacting residues.

The location of the phenyl group in the **6**–uPA complex makes it amenable to serve as a scaffold for substitution into other regions of the protein. Figure 2 indicates that space exists for substitution at meta and para positions, while ortho substitution would on one side run into the His99 side chain. Again, an attempt was made here to extend back toward S4 via ortho substitution, but compounds with that modification had greatly reduced activity, confirming the tight fit with the defining side wall of S2. In general, even small ortho substitution proved detrimental.⁴¹

A survey of meta and para substitution SAR is shown in Table 2. The *p*-aminomethyl compound **25** produced the greatest increase in potency and selectivity. The crystal structure of the **25**–uPA complex (Figure 2b) shows substantially the same overall structure as that of the parent amide **6**, with the core position and all relevant hydrogen bonds involving the amide of a very similar nature. The amide NH and Ser214 hydrogen-bond distances to the bridging water molecule for **25** are 3.0 and 2.8 Å, respectively, while the hydrogen-bond distance involving Gln192 is a much more normal 3.1 Å. The important additional feature for **25** is a salt bridge interaction between the Asp60A carboxylate O δ 2 and the charged amino group. The bond distance of 3.2 Å in the crystal structure is again within the expected range for such an interaction. The amino group is swung away from the protein surface in the X-ray structure, slightly increasing the distance from Asp60A O δ 2, probably in order to make it maximally available for stabilization by solvent. The structure of this complex shows a notable absence of well-defined water molecules binding to **25**; however, the relatively flat, nonpolar environment in the vicinity of the amino tail of **25** provides little in the way of a template for ordering solvent. In addition, we observed no ordered water molecules in this region in any of our inhibitor–uPA crystal structures, including the **6**–uPA complex, though a solvent-exposed water molecule with only one hydro-

Table 2. Acyclic Substitution and Disubstitution of Phenyl Ring

	R	K_i (nM) ^a					
		uPA	kallikrein	tPA	trypsin	plasmin	thrombin
6		631 ± 86	2500 ± 1140 (9)	31800 ± 17800 (9)	325 ± 175 (8)	1950 ± 580 (9)	564 ± 2160 (9)
25	4-CH ₂ NH ₂	40	7170 ± 2070	58400	2080 ± 400	16000 ± 900	>100000
28	4-CH ₂ OH	38.0 ± 4.2	2570	8350	260	3820	35100
31a	4-Et	736 ± 283	18100	83900	1320	3870	43700
31b	4-CONH ₂	326 ± 70	2430	>100000	235	1970	2350
34a	3-OMe	233 ± 8					
34b	3-OEt	82.0 ± 16.0	—	—	—	—	—
34c	3-O <i>i</i> Pr	63.0 ± 13.0	1370	2370	51	554	3490
34d	3-O(3-pentyl)	104 ± 1	—	—	—	—	—
34e	3-OCy ^b	28.0 ± 4.0	2720	3390	56	498	5580
34f	3-OPh	517 ± 94	—	—	—	—	—
34g	3-CH ₂ Cy ^b	167 ± 15	—	—	—	—	—
37a	3,5-OMe	139 ± 11	—	—	—	—	—
37b	3,5-O <i>i</i> Pr	28.0 ± 0.0	4300	790	13	1060	21700
37c	3-OCy, ^b 5-O <i>i</i> Pr	22.0 ± 4.0	3330	844	11	966	21600

^a ± standard deviation (number of determinations if more than two). All determinations are triplicate values. ^b Cy = cyclopentyl.

gen bond to protein is often not sufficiently ordered to appear in a crystal structure. However, the protonated amine almost certainly benefits from solvation by less well ordered water molecules. It is also important to note that the Asp60A carboxylate is not stabilized by any nearby positively charged or even uncharged hydrogen-bonding residues.

The interaction with Asp60A is particularly significant, as there is little sequence homology between other members of the trypsin family for this and nearby residues. Plasma kallikrein, for which there is not yet a solved crystal structure, possesses a Gly60A and a more distant Asp60 that might possibly lend some small electrostatic stabilization to a complex with **25**. Nevertheless, without generating a steric clash, the probable lack of a meaningful salt bridge or hydrogen-bonding interaction leads to a similar affinity toward kallikrein for **6** and **25**, resulting in an increase in selectivity for **25** from 4- to 180-fold (Table 2). Similarly, modeling **25** into the known tPA structure shows that the protein accommodates binding of **25** but again provides no stabilizing electrostatic interactions, resulting in an affinity near that of **6** and a consequent increase in selectivity. Trypsin, against which it is notoriously difficult to generate selectivity, is missing a five amino acid loop insertion between β -strands after residue 60, which contributes to its overall open, promiscuous structure; **25** nevertheless loses affinity toward trypsin, resulting in 50-fold selectivity against it. Modeling of **25** into plasmin, with a charge-paired Glu60 and Lys60A in the corresponding location, indicates that the presence of the aminomethyl group of **25** may cause a minor steric clash, which again may be responsible for the small loss in activity compared to **6**. Thrombin possesses a very large and rigid five amino acid loop insertion at residue 60, which greatly curtails the available space in this region. Consequently, thrombin is unable to bind to **25**, resulting in >2500:1 selectivity for uPA.

The hydroxymethyl analogue **28**, able to form a hydrogen bond but not a salt bridge with Asp60A, interestingly has essentially identical binding affinity

to urokinase. Somewhat surprisingly, the almost completely solvent-exposed salt bridge between Asp60A O δ 2 and **25** is only roughly equivalent in energy to the more typical hydrogen-bonding interaction with **28**. The ethyl derivative **31a** presents only a steric challenge and is accommodated with no change in binding energy to urokinase relative to **6**, but there is a small selectivity increase across the board. Roughly the same holds for the amide-substituted **31b**; modeling of this compound has demonstrated an inability of the amide to access a conformation allowing for an effective hydrogen bond; thus, toward urokinase, the effect of the group is reduced to a steric one. The affinities for **28**, **31a**, and **31b** toward the members of the selectivity panel are in almost all cases the same as or less than those for **6**. As steric issues are virtually identical for these three compounds as well as for **25**, we surmise that with the exception of thrombin, for which all of the compounds clash with the 60-loop insertion, the other enzymes are able to accommodate the added substituents, but these groups do not in any meaningful way interact with the protein surfaces. The slightly larger drop in affinities for **25** toward the panel members as a group is probably attributable to a small destabilization of the charged amino group upon moving from an aqueous to a partially surface-defined environment.

With the availability of cocrystals of urokinase with many of our compounds, we sought to identify additional, new subsites that were reachable from our scaffold and which might impart added activity and selectivity to our compounds. We became interested in two small dimples extending beyond the His57 imidazole toward the outer surface of the protein (Figure 2c). The first of these appeared readily accessible, leading us to seek a hydrophobic interaction with this region via substitution off the phenyl meta position. The series of ethers **34a–f** were made in an effort to explore this interaction. As seen from the binding data for this series (Table 2), urokinase affinity indeed increases with larger size up to the cyclopentyl ether of **34e**, with the exception of the 3-pentyl **34d**. It seems likely here that the additional entropic contribution associated with the

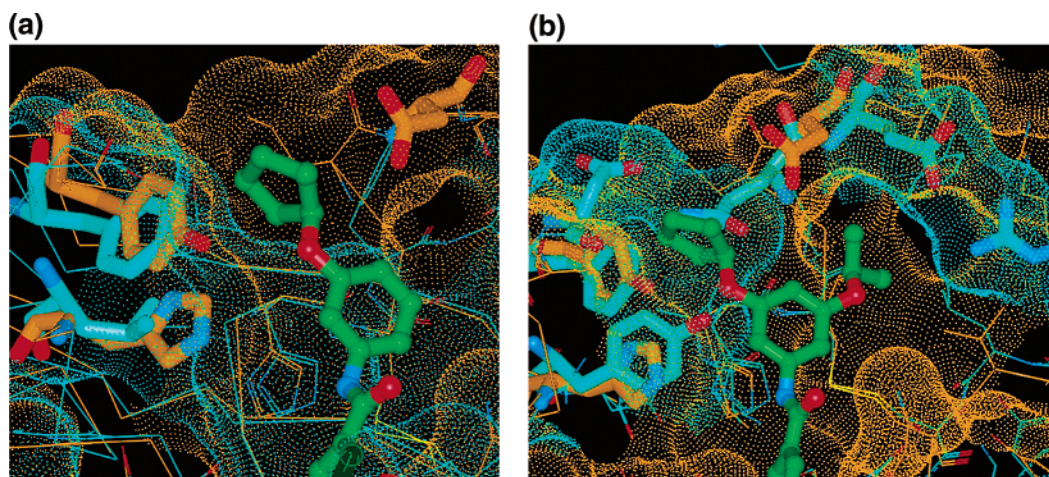


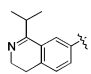
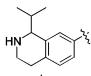
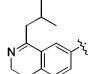
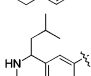
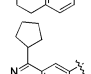
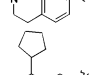
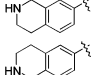
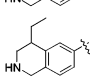
Figure 3. (a) Overlay of crystal structure of **34e** (green carbons) in urokinase (orange carbons and surface) with a crystal structure of trypsin (PDB entry 1EPT, blue carbons and surface). Residues Asp60A, Tyr94, and His99 of urokinase and Phe94 and Leu99 of trypsin are highlighted. The larger size of the dimple region is evident. (b) Model of **37c** (an OiPr was appended to the structure of **34e**) bound to urokinase (orange), with residues Asp60A, Tyr94, and His99 highlighted. A crystal structure of tPA (PDB entry 1RTF, blue) is overlaid with a dotted surface over highlighted residues (counterclockwise from right) Arg39, Glu60A, Gln60, Asp96, Phe94, and Tyr99. The dimple region of tPA clashes with the cyclopentyl ether, while the Arg39-Glu60A salt bridge truncates the prime-side protein binding cleft.

pentyl group relative to the cyclopentyl is responsible for the reduction in activity. In Figure 2c, the X-ray structure of the **34e**-uPA complex shows the floor of this dimple region primarily defined by the His57 backbone and the more prominent wall by the edge of the His99 imidazole. The small size of the surface dimple does not allow the cyclopentyl group to lie flat; instead, the ring is essentially edge-on, making an excellent fit with the urokinase surface. The alkyl ring is very well defined in the dimple region, with no apparent density at the other meta position in the crystal structure. A ring pucker was not assigned to the cyclopentyl group, due to presumed freedom of movement and typical uncertainties arising from the crystal structure. The *B* factors for the cyclopentyl carbon atoms were moderate to good, ranging from 24.65 to 26.15.

Other issues relating to the binding of **34e** were assessed through compounds **34f** and **34g**. The phenyl group in **34f** is roughly the same size as a cyclopentyl, but changing the aliphatic group to an aromatic group appears to provide little or no additional binding energy over that of **6**. Though this may demonstrate some preference of the dimple subsite for aliphatic residues, on closer inspection, given the small size of the dimple and the tight nature of the fit of the surface with **34e**, it is more likely that the change from an sp^3 to an sp^2 linking carbon atom keeps the phenyl group from adopting a position similar to the cyclopentyl ring of **34e**. Thus, the geometry of attachment does not allow an adequate test of the aromatic-for-aliphatic substitution. Next, the alkyl-substituted **34g** was made in an effort to probe the importance of the linking oxygen atom. Though the ether oxygen in Figure 2c appears to be in close contact with the protein surface, it was not clear whether a small movement of the inhibitor would be sufficient to allow a methylene enough room to serve as a substitute. In the event, the drop in affinity for **34g** makes it appear that the ether oxygen is important due to steric reasons, though we cannot rule out an electronic contribution of the ether regarding the interaction with the phenyl group and His57.

Selectivities also increase somewhat from **6** to **34c** to **34e**, dramatically so toward thrombin, which again suffers from the interference of its 60-loop insertion. In particular, modeling of **34e** into thrombin gives evidence of a prohibitive clash with Tyr60A. While for the other four enzymes there is an initial boost in affinity for the isopropoxy **34c**, the larger **34e** produces a drop, or no further gain, in affinity. Plasmin, with its characteristic lack of a defined subsite, and kallikrein pick up little binding energy, improving by 4-fold and remaining constant, respectively. Though the active site His57 is a conserved residue, the dimple-forming His99 is a unique residue for urokinase among trypsin-like serine proteases. Again, as there are no available X-ray structures of plasma kallikrein, which possesses a Gly99, we cannot with complete confidence assert that this change drives the increases in selectivity for the ethers; however, other enzymes in this family tend to have the same secondary structure in this region. Known crystal structures of trypsin and tPA, then, possess the same dimple region, but the dimples take different forms. Trypsin possesses a larger dimple subsite, with the identities of key residues changed (Figure 3a). His99 in urokinase becomes Leu99 in trypsin, and additionally, Tyr94 becomes Phe94; in both cases the slightly smaller residues of trypsin are nearly superimposable on the corresponding urokinase residues. The result is a looser fit with the isopropyl and cyclopentyl groups. In the event, **34c** and **34e** experience a 6-fold gain in affinity to trypsin, compared to 10- and 22-fold gains toward urokinase, producing a reversal in selectivity from 1:2 to 2:1. In the case of tPA, residue 99 becomes a tyrosine, leading to a much smaller dimple subsite and a clash with the larger **34e** (Figure 3b). While tPA, like trypsin, has a smaller Phe94 rather than a tyrosine, it also has a Gln60 residue whose side chain projects into the space defined in the urokinase structure by Leu60. In Figure 3b, the bis-ether **37c**, based on the crystal structure of **34e**, is shown modeled into a tPA structure. The figure illustrates the clash with the cyclopentyl group. The opposite meta position,

Table 3. Cyclic Substitution of Phenyl Ring

R	K _i (nM) ^a						
	uPA	kallikrein	tPA	trypsin	plasmin	thrombin	
6	Ph	631 ± 86	2500 ± 1140(9)	31800 ± 17800(9)	325 ± 175(8)	1950 ± 580(9)	564 ± 2160(9)
25	CH ₂ NH ₂	40	7170 ± 2070	58400	2080 ± 400	16000 ± 900	>100000
43a		48.0 ± 1.0	436	1840	42	768	4990
47a		23.5 ± 0.7	230	1120	43	631	5720
43b		161 ± 23	-	-	-	-	-
47b		123 ± 1	1350	>50000	115	1190	7310
43c		35.5 ± 1.1	849	3130	58	765	5310
47c		26.5 ± 2.1	400	3950	39	833	10160
56b		16.5 ± 6.0	112	2320	92	1030	6920
56a		6.3 ± 0.1	145	1650	82	1120	6440

^a ± standard deviation (number of determinations if more than two). All determinations are triplicate values.

however, presents a pocket with room for an isopropyl or even a cyclopentyl group. It seems likely based on this and other data, discussed below, that the monoether series **34a–g** binds to tPA in this reverse sense, at least for those inhibitors possessing larger substituents.

For urokinase, extending out in this opposite direction from the dimple region is the very broad, shallow, prime-side protein binding groove, immediately defined by Tyr60B and Gln192, with the floor of the groove defined by Val41 and the Cys42–Cys58 disulfide bond (see Figure 2a–c). We sought to extend our ether inhibitors into this cleft by synthesizing and testing the series of bis-ethers **37a–c**, designed to have one alkyl group anchored into the dimple region with the other exploring the broader cleft. Comparing **34a,c,e** to **37a–c**, we find small improvements in affinity to uPA, while compounds were slightly less active against kallikrein and plasmin and much less active against thrombin. The second ether substituent seemed to significantly improve binding to tPA and trypsin, however.

It is straightforward enough to rationalize the measured affinities of **37b** and **37c** for thrombin, which again experiences a clash due to its 60-loop insertion. Also, for urokinase, kallikrein, and plasmin, the inhibitors evidently fail to generate much additional binding energy by making close contact with the protein surfaces, instead fitting more loosely into the prime-side cleft and picking up a small binding increment by displacing disordered water molecules.⁴² Explanation of the improvements seen toward tPA and trypsin, however, are less clear. Returning to Figure 3b, tPA exhibits an interesting difference in prime-side architecture, with Arg39 and Glu60A forming a salt bridge that truncates the normally broad and poorly defined protein binding cleft. As discussed above, this may allow for close contact between tPA and the isopropyl or cyclo-

pentyl ethers. The second, smaller ether may then be accommodated on top of the less well defined, smaller dimple region, picking up an additional 4-fold gain in binding. On the basis of the binding data for **34c** and **34e** and for **37b,c**, the isopropyl and cyclopentyl groups are roughly equivalent. Again, it seems likely that the cyclopentyl group, which is much more difficult to accommodate in the dimple subsite, will choose to go into the prime-side cleft.

The improved binding of the bis-ethers to trypsin is more difficult to rationalize. Trypsin crystal structures display the more typical broad prime-side binding cleft, and close contacts are not apparent; it is thus not obvious where additional binding energy might be generated. We cannot rule out the possibility of an electronic effect involving added electron density to the phenyl ring, though again, this should affect binding to all of the enzymes through the conserved His57 residue.

The 1-alkyl di- and tetrahydroisoquinoline series **43a–c** and **47a–c** also extend alkyl groups into the protein binding groove. The imine and amine functionalities were included to interact with the Asp60A side chain. For both series, the rank ordering of compounds with respect to activity is isobutyl < isopropyl ≤ cyclopentyl (Table 3), with the latter two groups resulting in potencies equal to or better than **25** and selectivities increasing incrementally as a group. Figure 4a shows the X-ray structures of the two isopropyl compounds bound to urokinase. Both **43a** and **47a** place the isopropyl group in the middle of the prime-side cleft between Tyr60B and Gln192. As seen with **37b** and **37c**, neither alkyl group makes a strong hydrophobic protein–inhibitor contact. Given the small size of the energy gain associated with the alkyl groups, we surmise that this gain results from the displacement of what are likely loosely bound, relatively disordered water molecules

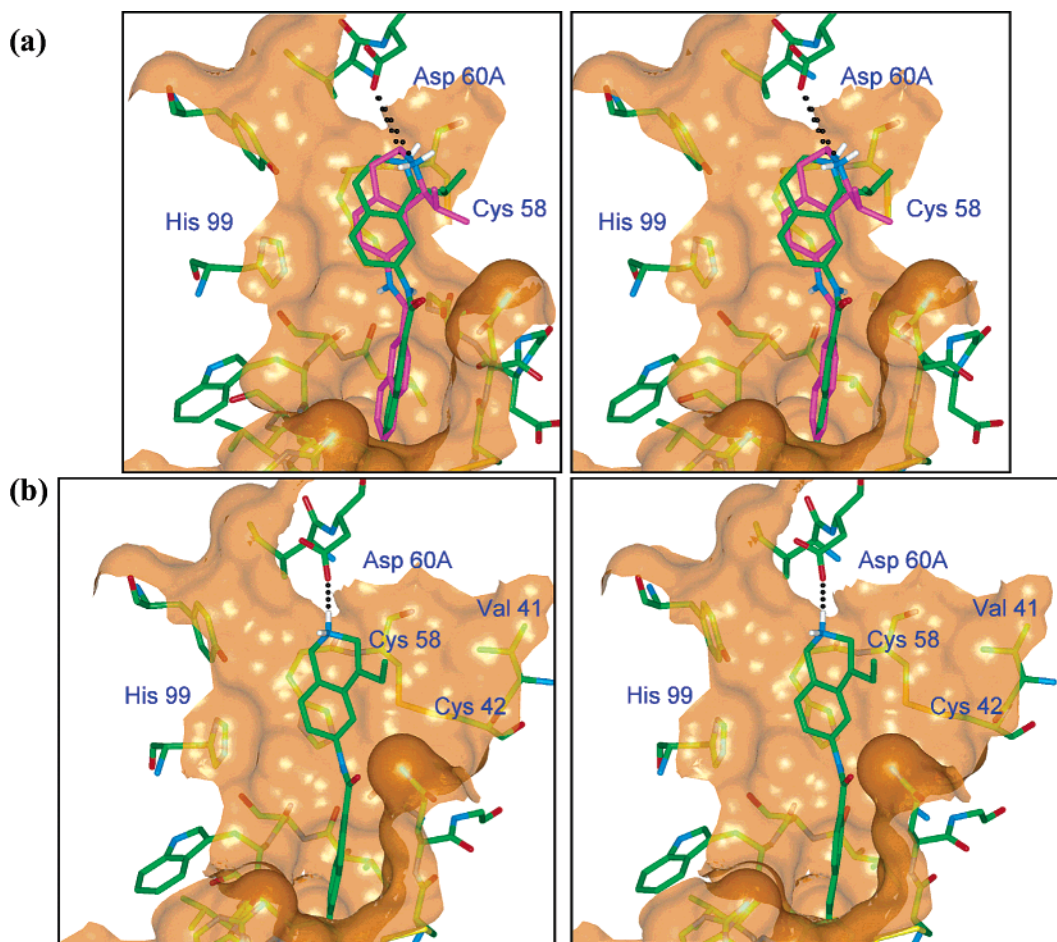


Figure 4. Stereoviews of substituted amides in crystal structures of uPA complexes, with Connolly surfaces. (a) **43a** (green) and **47a** (red) bound to uPA, showing relatively long contacts (dotted lines) with Asp60A, and isopropyl groups situated above the Cys58-Cys42 disulfide bridge, pointing into the water-filled protein binding region of protein, away from the surface. For **47a**, the density for the *R*-enantiomer, with the isopropyl group pointing toward the surface, is not seen. Hydrogen bonds to Gln192 N ϵ 2, omitted for clarity, are 3.6 and 3.1 Å, respectively. (b) **56a** bound to uPA. Excellent contact is made with Asp60A, with the ethyl group again pointing into the protein binding cleft. Again, density for the *R*-enantiomer is not seen.

normally filling the cleft. The net benefit is then due to entropy contributions, which are small when the displaced water molecules were originally weakly bound near the protein surface.⁴² Recently published work has shown this region to be potentially fruitful in providing additional binding energy toward urokinase,^{23a} however, due to the seeming preference for our scaffolds to extend substituents toward solvent, we were unable to achieve a significant hydrophobic interaction with the exocyclic alkyl groups.

We can infer, based on the data for **43a–c**, **47a–c**, and the bis-ethers above, that the intrinsic affinities of the di- and tetrahydroisoquinolines without the exocyclic alkyl groups are almost certainly less than for **25**. This is in keeping with the far less ideal interactions with Asp60A. With the basic nitrogens moved one atom farther away, the imino group of **43a** is 3.3 Å from Asp60A O δ 2, while the **47a** amine nitrogen distance is 3.8 Å. The imine of **43a**, with only one hydrogen in its protonated form, has its hydrogen-bonding capacity satisfied by the Asp60A O δ 2 interaction, while the protonated amine of **47a** can still benefit from extending into solvent. The saturated ring containing the amine of **47a** is puckered outward at the nitrogen, projecting the amine farther out into solvent and farther away from Asp60A O δ 2; the increased distance to the car-

boxylate is probably balanced by better solvation by water. This is similar to the behavior of **25**, where the primary amine has even more driving force favoring solvation. Interestingly, the X-ray structure of **47a** shows density only for the *S*-stereoisomer, which at the resolution of the structure in question indicates at least a 10-fold difference in affinity between the two enantiomers. The observed ring pucker would have the isopropyl group of the *R*-enantiomer pointing straight down and clashing with the urokinase surface, resulting in the bias toward the *S*-enantiomer.

We should expect selectivity trends for **43a–c** and **47a–c** to roughly mirror those for **37a** and **37b**, being driven by the alkyl substituents off of the ring system. These alkyl groups are approximately superimposable with the second ether groups of **37a** and **37b** when protein-bound; however, not having the flexible oxygen linking atom, their range of possible vectors is limited. While no unsubstituted di- and tetrahydroquinolines were synthesized to provide points of comparison for members of the series, within the two groups there is a general lack of discernible trends in affinities. Again, with the exception of thrombin and its 60-loop, the inhibitors seem to fail to produce a reasonable fit with the broad, flat surface of the binding clefts, resulting in equally flat SAR. The affinities to tPA are of note,

however, as while the initial gains from the isopropyl substituents in **43a** and **47a** are more substantial than those for the other proteases, it appears that the cyclopentyl substituents, and certainly the isobutyl group in **47b**, are too large to be accommodated by the prime-side cleft. In Figure 3b the alkyl ether is permitted to extend toward the Arg39-Glu60A salt bridge, but here the alkyl groups are aimed toward the narrow cleft extending alongside and beyond Arg39. This region is much smaller and would likely not be able to fit an isobutyl group. Thus, though the insertion of the salt bridge might be responsible for the greater initial gain in affinity to tPA, it also accounts for the greater sensitivity toward larger or less optimally situated substituents.

The final compounds in Table 3, the 6-linked tetrahydroisoquinolines **56a** and **56b**, were designed to interact with the Asp60A carboxylate in identical fashion to **25**, while gaining additional affinity from extension into S1'. The unsubstituted **56b** gains a small increment of affinity relative to **25**, though there is a notable loss of selectivity across the panel of enzymes. Alkyl substitution in the form of the ethyl compound **56a** produces the now familiar small increase in activity to $K_i = 6$ nM, with 2–3-fold improvements in selectivity against all five enzymes in the panel. The gross structure of the complex in the crystal structure is similar to those discussed above, with a 2.9 Å hydrogen bond to Gln192 and a water-mediated hydrogen bond from the amide to Ser214 with distances of 3.3 and 2.8 Å. In Figure 4b, the ethyl derivative **56a** is shown binding to urokinase with a near optimal geometry of interaction with Asp60A O δ 2. The placement of the amino group is necessarily much closer to the urokinase surface than for the acyclic **25**. The potential for interaction with water is thus reduced, with the remaining amine hydrogen pointed directly into water, available for solvation. Thus, combination of a near-optimized hydrogen-bonding geometry with the benefit accruing from additional hydrophobic scaffolding has led to a single-digit nanomolar urokinase inhibitor.

One aspect of our inhibitor data that is somewhat difficult to clearly understand is the precise identification of the driving force for the outstanding selectivity of **25**. While many compounds engage Asp60A O δ 2 with suboptimal geometry, many also derive small contributions to selectivity from alkyl substituents. Nevertheless, **25** achieves overwhelming selectivity advantages over our other compounds. Ignoring the various alkyl substituents, and comparing **25** to **56b**, selectivity seems to be correlated with hydrogen-bonding capacity and the extent of stabilization provided by the Asp60A carboxylate. Specifically, the embedding of the amino group of **25** into the ring system of **56b** produces a much smaller energy gain for binding to urokinase than to the members of the selectivity panel, in particular kallikrein and trypsin. The known crystal structures of these proteases offer no clues as to other factors that may be involved in the binding events of these inhibitors. In the absence of X-ray data for these other inhibitor–enzyme complexes, we can only speculate that the well-documented reduced desolvation cost for a secondary amine as compared to a primary amine impacts less on urokinase affinities because of the

presence of the Asp60A carboxylate, which offers a great deal of charge stabilization on its own. Nevertheless, it seems likely that enthalpic and entropic differences between bound and unbound enzyme–inhibitor states must be partly driven by solvent contributions. The effects on naphthamidine urokinase inhibitors of combination of this substituent interaction and the hydrophobic interactions discussed above, along with those of substituents at position 8, will be reported in due course.

Conclusion

Our research into 2-naphthamidines as uPA inhibitors has previously demonstrated the utility of the core as a scaffold from which adding substituents at the 8 position can result in increased potency and selectivity. By starting from the amide **6**, using structure-based design, we have been able to identify and access three new points of interaction, again leading to improved potency and selectivity. One interaction involves making a salt bridge or hydrogen bond with O δ 2 of Asp60A, a residue unique to urokinase among trypsin-like serine proteases. Another interaction involves a hydrophobic close contact with a small dimple on the protein surface primarily defined by His57 and His99. Finally, we have accessed the prime-side protein binding groove, where small improvements in potency and selectivity are gained through displacement of water molecules with alkyl groups. Potency gains through these interactions have resulted in compounds with K_i values as low as 6 nM, displaying a 1000-fold improvement in activity over 2-naphthamidine. Many compounds also achieved excellent selectivity against other trypsin-like serine proteases. Through combination of this work with efforts investigating 8-substitution of 2-naphthamidines, more fully elaborated, disubstituted naphthamidine urokinase inhibitors accessing multiple binding sites and possessing improved binding should be generated. Application to other scaffolds of our work identifying these new binding subsites may also help lead to improved inhibitors of urokinase.

Experimental Section

General Methods. All reactions were carried out under inert atmosphere (N_2) and at room temperature unless otherwise noted. Solvents and reagents were obtained commercially and were used without further purification. All reported yields are of isolated products and are not optimized. 1H NMR spectra were obtained on a Nicolet QE-300 (300 MHz) or a General Electric GN-300 (300 MHz) instrument. Chemical shifts are reported as δ values (ppm) downfield relative to Me_4Si as an internal standard, with multiplicities reported in the usual manner. Mass spectra determinations were performed by the Analytical Research Department, Abbott Laboratories; DCI/ NH_3 indicates chemical ionization in the presence of ammonia, ESI indicates electron spray ionization, and APCI indicates atmospheric pressure chemical ionization with ammonia. Elemental analyses were performed by Robertson Microlit Laboratories, Inc., Madison, NJ. Column chromatographies were carried out in flash mode on silica gel (Merck Kieselgel 60, 230–400 mesh). Preparative HPLC purification was carried out on a Pharmacia Biotech HPLC with p-50 pump and a C18 column (40 micron, 30 \times 2 cm, J.T. Baker), with UV detection at 250 nm and solvent mixtures in a gradient ranging from 90% A (0.1% aqueous TFA)/10% B (CH_3CN or MeOH) to 10% A/90% B over 160 min at a flow rate of 5 mL/min [fractions were collected every 2 min for 100 min and analyzed by TLC (10:1:1 acetonitrile/water/acetic acid) for

product]. Purification methods for individual final products are noted, and all physical data for final compounds correspond to the indicated salt form.

6-Carbomethoxy-2-naphthalenecarboxylic Acid (8). A suspension of dimethyl 2,6-naphthalenedicarboxylate **7** (50 g, 204 mmol) in dioxane (300 mL) was heated at 80 °C until all solid dissolved, slowly treated with a solution of KOH (13.2 g, 210 mmol) in MeOH (10 mL), stirred for an additional 2 h at 80 °C, cooled to room temperature, and filtered, and a solid residue was rinsed with ether. The solid was dissolved in water and treated with 2 M HCl to pH 3, and the precipitate was filtered, washed with water, and dried under vacuum to provide 45.2 g (96%) of **8** as a white powder: ¹H NMR (DMSO-*d*₆) δ 13.24 (br s, 1H), 8.68 (s, 1H), 8.66 (s, 1H), 8.23 (d, *J* = 8.6 Hz, 2H), 8.04 (d, *J* = 8.6 Hz, 2H), 3.92 (s, 3H); MS (DCI/NH₃) *m/z* 231 (M + H)⁺.

6-Carbamyl-2-naphthalenecarboxylic Acid, Methyl Ester (9). A suspension of **8** (15 g, 65 mmol) in toluene (190 mL) was treated with SOCl₂ (20 mL, 276 mmol) and DMAP (15 mg, 0.123 mmol) and refluxed for 1 h. Excess SOCl₂ and 60 mL of solvent were then removed by distillation. The thick precipitate which formed while cooling to room temperature was triturated with hexanes and filtered. The solid was dissolved in CH₂Cl₂ (400 mL) at room temperature and was treated with dry ammonia gas to precipitate the product. The mixture was stirred for an additional 15 min, filtered, and dried under vacuum to yield 13.3 g (89%) of **9** as a white powder: ¹H NMR (DMSO-*d*₆) δ 8.69 (s, 1H), 8.56 (s, 1H), 8.24 (s, 1H), 8.22 (d, *J* = 8.5 Hz, 1H), 8.14 (d, *J* = 8.5 Hz, 1H), 8.04 (d, *J* = 8.5 Hz, 2H), 7.60 (s, 1H), 3.94 (s, 3H); MS (DCI/NH₃) *m/z* 230 (M + H)⁺.

6-Cyano-2-naphthalenecarboxylic Acid, Methyl Ester (10). To a solution of **9** (39.9 g, 174 mmol) and pyridine (28.2 mL, 350 mmol) in dioxane (200 mL) at 0 °C was added dropwise TFAA (40.2 g, 192 mmol), and the reaction was stirred for 3 h at room temperature. The reaction was then poured into water and extracted with EtOAc (3 × 150 mL), and the combined extracts were washed with water (4 × 100 mL), dried (MgSO₄), and condensed to provide 34.7 g (94%) of **10**: ¹H NMR (CDCl₃) δ 8.64 (s, 1H), 8.27 (s, 1H), 8.19 (dd, *J* = 8.5, 1.5 Hz, 1H), 8.04 (d, *J* = 8.9 Hz, 1H), 7.96 (d, *J* = 8.9 Hz, 1H), 7.68 (d, *J* = 8.5, 1.7 Hz, 1H), 4.01 (s, 3H); MS (DCI/NH₃) *m/z* 212 (M + H)⁺.

6-Cyano-2-naphthalenecarboxylic Acid (11). Compound **10** (1.9 g, 9 mmol) in 1:1 THF/H₂O (40 mL) was treated with LiOH·H₂O (1.9 g, 45 mmol), stirred for 90 min, and concentrated to a thick slurry. The slurry was dissolved in 1 M HCl (100 mL) and extracted with EtOAc (3 × 250 mL). The combined organic extracts were washed with brine, dried (Na₂SO₄), filtered, and concentrated to provide 1.6 g (99%) of **11** as a white solid: ¹H NMR (CDCl₃) δ 13.38 (br s, 1H), 8.72 (s, 1H), 8.68 (s, 1H), 8.34 (d, *J* = 8.9 Hz, 1H), 8.17 (d, *J* = 8.5, Hz, 1H), 8.12 (dd, *J* = 8.5, 1.4 Hz, 1H), 7.90 (dd, *J* = 8.5, 1.6 Hz, 1H); MS (DCI/NH₃) *m/z* 198 (M + H)⁺.

6-Cyano-2-naphthalenecarbonyl Chloride (12). A suspension of **11** (1.4 g, 7.1 mmol) in toluene (50 mL) was treated with (COCl)₂ (0.93 mL), heated at 70 °C for 18 h, treated with additional (COCl)₂ (0.5 mL), heated at 70 °C for 4 h, condensed, and condensed twice more from toluene to provide 1.52 g (99%) of **12**: ¹H NMR (CDCl₃) δ 8.79 (s, 1H), 8.32 (s, 1H), 8.17 (dd, *J* = 8.9, 1.8 Hz, 1H), 8.13 (d, *J* = 8.9 Hz, 1H), 8.03 (d, *J* = 8.9 Hz, 1H), 7.77 (dd, *J* = 8.9, 1.5 Hz, 1H); MS (DCI/NH₃) *m/z* 216 (M + H)⁺.

6-(*N*-Phenylcarbamyl)-2-naphthalenecarbonitrile (13a). A solution of **11** (930 mg, 4.72 mmol) and *i*Pr₂NEt (1.64 mL, 9.44 mmol) in DMF (40 mL) at 0 °C was treated with HATU (1.79 g, 4.72 mmol), stirred for 30 min at 0 °C, treated with aniline (473 μL, 5.19 mmol), and stirred for 18 h. The mixture was poured into water (400 mL), extracted with EtOAc (3 × 250 mL), washed with water and brine, dried (Na₂SO₄), filtered, and concentrated to provide a yellow oil which was flash chromatographed on silica gel eluting with 25% EtOAc/hexanes to provide 567 mg (44%) of **13a**: ¹H NMR (CDCl₃) δ 8.43 (s, 1H), 8.30 (d, *J* = 1.5 Hz, 1H), 8.06 (d, *J* = 8.9 Hz, 1H),

8.05 (m, 2H), 7.95 (br s, 1H), 7.71 (d, *J* = 8.9 Hz, 1H), 7.68 (d, *J* = 8.5 Hz, 1H), 7.42 (dd, *J* = 8.5, 8.4 Hz, 1H), 7.21 (t, *J* = 8.4 Hz, 1H); MS (DCI/NH₃) *m/z* (M + H)⁺ 273.

6-(*N*-Phenylcarbamyl)-2-naphthalenecarboxamide (6). A solution of **13a** (52 mg, 0.191 mmol) in THF (2 mL) was treated with 1 M LiN(TMS)₂ in THF (0.6 mL), stirred for 18 h, treated with 2 M HCl (4 mL), stirred for another 24 h, basified with saturated Na₂CO₃, and extracted with EtOAc (3 × 10 mL). The extracts were washed with brine, dried (Na₂SO₄), filtered, and concentrated. The crude product was converted to the CH₃SO₃H salt to provide 15 mg (20%) of **6**: ¹H NMR (DMSO-*d*₆) δ 10.56 (s, 1H), 9.50 (br s, 2H), 9.09 (br s, 2H), 8.69 (s, 1H), 8.54 (s, 1H), 8.33 (d, *J* = 8.8 Hz, 1H), 8.25 (d, *J* = 8.8 Hz, 1H), 8.16 (dd, *J* = 8.8, 1.7 Hz, 1H), 7.90 (dd, *J* = 8.5, 1.7 Hz, 1H), 7.83 (d, *J* = 8.2 Hz, 2H), 7.40 (dd, *J* = 8.2, 7.5 Hz, 2H), 7.14 (t, *J* = 7.5 Hz, 1H), 2.32 (s, 3H); MS (DCI/NH₃) *m/z* 290 (M + H)⁺. Anal. (C₁₈H₁₆N₃O·CH₃SO₃H·0.5H₂O) C, H, N.

6-(*N*-Phenyl-*N*-methylcarbamyl)-2-naphthalenecarbonitrile (13b) was prepared from **11** and *N*-methylaniline using the procedure described for the preparation of **13a**: ¹H NMR (DMSO-*d*₆) δ 8.50 (s, 1H), 8.03 (d, *J* = 1.5 Hz, 1H), 8.00 (d, *J* = 8.5 Hz, 1H), 7.87 (d, *J* = 8.5 Hz, 2H), 7.76 (dd, *J* = 8.5, 1.7 Hz, 1H), 7.49 (dd, *J* = 8.5, 1.5 Hz, 1H), 7.23 (m, 5H), 3.44 (s, 3H); MS (DCI/NH₃) *m/z* 287 (M + H)⁺.

6-(*N*-Phenyl-*N*-methylcarbamyl)-2-naphthalenecarboxamide (14) was prepared from **13b** using the procedure described for the preparation of **6**. The crude product was purified by HPLC to provide **14**: ¹H NMR (DMSO-*d*₆) δ 9.42 (br s, 4H), 8.39 (s, 1H), 8.03 (d, *J* = 8.4 Hz, 1H), 7.99 (s, 1H), 7.90 (d, *J* = 8.4 Hz, 1H), 7.78 (dd, *J* = 8.5, 1.7 Hz, 2H), 7.48 (d, *J* = 8.5 Hz, 1H), 7.22 (m, 4H), 7.11 (m, 1H), 3.45 (s, 3H); MS (DCI/NH₃) *m/z* 304 (M + H)⁺. Anal. (C₁₉H₁₇N₃O·C₂H₅HF₃O₂) C, H, N: calcd, 10.07; found, 9.64.

6-(*N*-Methylcarbamyl)-2-naphthalenecarbonitrile (13c) was prepared from **11** and methylamine using the procedure described for the preparation of **13a**: ¹H NMR (DMSO-*d*₆) δ 8.74 (br q, 1H), 8.64 (s, 1H), 8.53 (s, 1H), 8.22 (d, *J* = 8.8 Hz, 1H), 8.15 (d, *J* = 8.8 Hz, 1H), 8.06 (dd, *J* = 8.6, 1.7 Hz, 1H), 7.86 (dd, *J* = 8.5, 1.8 Hz, 2H), 2.86 (d, *J* = 4.4 Hz, 3H); MS (DCI/NH₃) *m/z* 228 (M + NH₄)⁺.

6-(*N*-Methylcarbamyl)-2-naphthalenecarboxamide (15) was prepared from **13c** using the procedure described for the preparation of **6**. The crude product was purified by HPLC to provide **15**: ¹H NMR (DMSO-*d*₆) δ 9.42 (br s, 4H), 8.65 (br q, *J* = 4.8 Hz, 1H), 8.54 (m, 2H), 8.25 (d, *J* = 8.8 Hz, 1H), 8.17 (s, 1H), 7.90 (d, *J* = 8.8 Hz, 1H), 8.07 (dd, *J* = 8.4, 1.7 Hz, 2H), 7.88 (dd, *J* = 8.6, 1.8 Hz, 1H), 2.86 (d, *J* = 4.8 Hz, 3H); MS (DCI/NH₃) *m/z* 228 (M + H)⁺. HRMS (FAB) calcd, 228.1137; found, 228.1142.

6-(*N*-Methoxy-*N*-methylcarbamyl)-2-naphthalenecarbonitrile (16). A solution of **12** (1.5 g, 6.96 mmol) and CH₂-Cl₂ (30 mL) was added dropwise to a 0 °C solution of *N*,*O*-dimethylhydroxylamine hydrochloride (0.68 g, 6.96 mmol), Et₃N (2.4 mL, 17.4 mmol), and CH₂Cl₂ (40 mL). The reaction mixture was stirred for 15 min at 0 °C and for 2.5 h at room temperature and then was diluted with CH₂Cl₂; washed with 1 M KOH, 1 M HCl, water, and brine; dried (MgSO₄); filtered; and condensed to yield 1.6 g (96%) of **16** as a white solid: ¹H NMR (CDCl₃) δ 8.26 (s, 2H), 8.00 (d, *J* = 8.5 Hz, 1H), 7.94 (d, *J* = 8.9 Hz, 1H), 7.87 (dd, *J* = 8.9, 1.5 Hz, 1H), 7.67 (dd, *J* = 8.5, 1.5 Hz, 1H), 3.55 (s, 3H), 3.43 (s, 3H); MS (DCI/NH₃) *m/z* 241 (M + H)⁺.

6-(1-Oxo-2-phenylethyl)-2-naphthalenecarbonitrile (17). Benzylmagnesium chloride (2 M solution in THF, 1.2 mL, 2.4 mmol) was added dropwise to a 0 °C solution of **16** (200 mg, 0.8 mmol) in THF (10 mL). The reaction mixture was stirred for 0.5 h at 0 °C and then quenched with 1 M HCl and extracted with ether (2 × 30 mL). The extracts were washed with brine, dried (MgSO₄), filtered, and condensed, and the residue was flash chromatographed on silica gel eluting with 5% EtOAc/hexanes, followed by crystallization from hexanes/EtOAc to afford 60 mg (28%) of **17** as a white solid: ¹H NMR (CDCl₃) δ 8.55 (s, 2H), 8.26 (s, 1H), 8.17 (dd, *J* = 8.5, 1.7 Hz,

1H), 8.06 (d, $J = 8.5$ Hz, 1H), 7.97 (d, $J = 8.5$ Hz, 1H), 7.69 (dd, $J = 8.5, 1.7$ Hz, 1H), 7.33 (m, 5H), 4.42 (s, 2H); MS (DCI/NH₃) m/z 289 (M + NH₄)⁺.

6-(1-Oxo-2-phenylethyl)-2-naphthalenecarboxamide (18). Compound **17** (60 mg, 0.22 mmol) in MeOH (20 mL) at 0 °C was saturated with HCl gas, and the reaction was capped, stirred for 18 h, and concentrated to provide an off-white solid. The solid was treated with NH₄OAc (77 mg, 1 mmol) in MeOH (10 mL), heated at 40 °C for 15 h, cooled, and concentrated to a yellow solid. The residue was purified by HPLC to afford 30 mg (34%) of **18** as a white solid: ¹H NMR (DMSO-*d*₆) δ 9.50 (s, 2H), 9.16 (s, 2H), 8.93 (s, 1H), 8.53 (s, 1H), 8.38 (d, $J = 8.8$ Hz, 1H), 8.22 (d, $J = 8.8$ Hz, 1H), 8.17 (dd, $J = 8.8, 1.7$ Hz, 1H), 7.91 (dd, $J = 8.8, 1.7$ Hz, 1H), 7.34 (s, 2H), 7.33 (s, 2H), 7.26 (m, 1H), 4.57 (s, 2H); MS (ESI) m/z 289 (M + H)⁺. Anal. (C₁₉H₁₆N₂O·C₂HF₃O₂·0.5H₂O) C, H, N.

6-Azidocarbonyl-2-naphthalenecarbonitrile (19). To a solution of **12** (7.0 g, 32.5 mmol) in acetone (200 mL) was added a solution of NaN₃ (10.6 g, 163 mmol) in water (100 mL). The mixture was stirred for 90 min, and the precipitated product was filtered, washed thoroughly with water, and dried in a vacuum to yield 6.5 g (90%) of **19** as an off-white solid: ¹H NMR (CDCl₃) δ 8.64 (s, 1H), 8.28 (s, 1H), 8.16 (dd, $J = 8.6, 1.5$ Hz, 1H), 8.07 (d, $J = 8.5$ Hz, 1H), 7.98 (d, $J = 8.6$ Hz, 1H), 7.71 (dd, $J = 8.5, 1.5$ Hz, 1H); MS (DCI/NH₃) m/z 223 (M + H)⁺.

6-Amino-2-naphthalenecarbonitrile (20). To a solution of concentrated H₂SO₄ (45 mL) at 0 °C was added **19** (6.5 g, 29.2 mmol) and gas evolution immediately commenced. After 30 min at 0 °C the reaction mixture was warmed to room temperature, stirred for 30 min, poured into ice, and carefully neutralized with 50% NaOH solution. The solid product was filtered, washed with water, and dried under vacuum to yield 3.3 g (67%) of **20** as a light yellow solid: ¹H NMR (CDCl₃) δ 8.04 (s, 1H), 7.69 (d, $J = 8.6$ Hz, 1H), 7.60 (d, $J = 8.5$ Hz, 1H), 7.46 (dd, $J = 8.5, 1.5$ Hz, 1H), 7.02 (dd, $J = 8.6, 2.2$ Hz, 1H), 6.95 (d, $J = 2.2$ Hz, 1H); MS (DCI/NH₃) m/z 169 (M + H)⁺.

6-Benzoylamino-2-naphthalenecarbonitrile (21). To a solution of **20** (280 mg, 1.7 mmol) in a mixture of dioxane (50 mL) and 10% K₂CO₃ (15 mL) was added benzoyl chloride (400 μ L, 3.5 mmol). After 10 min the reaction mixture was quenched with *N,N*-dimethylethylenediamine (2 mL) and stirred for 10 min. The reaction mixture was diluted with EtOAc (100 mL) and water (50 mL) and separated, and the organic phase was washed with 1 M HCl (60 mL), water, and brine; dried (MgSO₄); filtered; and condensed. The resulting solid was treated with a solution of 1:1 ether/hexane and filtered and dried under vacuum to yield 154 mg (34%) of **21** as a white solid: ¹H NMR (DMSO-*d*₆) δ 8.57 (s, 1H), 8.09 (d, $J = 8.8$ Hz, 1H), 8.03 (d, $J = 8.8$ Hz, 1H), 7.98 (d, $J = 2.0$ Hz, 1H), 7.80 (m, 2H), 7.75 (m, 2H), 7.50 (d, $J = 7.1$ Hz, 1H), 7.43 (m, 2H); MS (DCI/NH₃) m/z 273 (M + H)⁺.

6-Benzoylamino-2-naphthalenecarboxamide (22). To a solution of **21** (157 mg, 0.58 mmol) in 10:1 pyridine/Et₃N (8 mL) was bubbled H₂S gas for 5 min, and the green solution was stirred overnight. EtOAc was added (100 mL) and the solution was washed with water (2 × 30 mL), followed by 1% aqueous citric acid and brine, dried (MgSO₄), filtered, and condensed. The crude product was treated with a mixture of ether (15 mL) and hexane (5 mL), and the resulting product was filtered, washed with ether and hexane, and dried in a vacuum to yield the thioamide. To the resulting yellow solid in acetone (20 mL) was added MeI (1.5 mL) and the mixture stirred for 3 h, after which the precipitated imidate thioester HI salt was collected by filtration. The salt was suspended in MeOH (10 mL), to which was added NH₄OAc (770 mg, 10 mmol), and the reaction was stirred overnight. The product was purified by HPLC to yield 84 mg (36%) of **22**: ¹H NMR (DMSO-*d*₆) δ 10.67 (s, 1H), 9.22 (br s, 4H), 8.65 (d, $J = 1.5$ Hz, 1H), 8.43 (d, $J = 1.4$ Hz, 1H), 8.10 (d, $J = 9.2$ Hz, 2H), 8.04 (m, 3H), 7.80 (dd, $J = 8.8, 1.8$ Hz, 1H), 7.61 (m, 3H); MS (ESI) m/z 290 (M + H)⁺. Anal. (C₁₈H₁₅N₃O·C₂HF₃O₂) C, H, N.

(4-tert-Butoxycarbonylmethyl)aniline (23b). 4-Aminomethylaniline **23a** (2.00 g, 16.4 mmol) in 2:1 THF/water

(30 mL) was treated with di-*tert*-butyl dicarbonate (3.93 g, 18 mmol), stirred for 18 h, diluted with water, and concentrated to a white slurry. The slurry was dissolved in EtOAc, washed with water and brine, dried (Na₂SO₄), filtered, and concentrated to provide 2.40 g (66%) of **23b** as a yellow solid: ¹H NMR (CDCl₃) δ 7.88 (d, $J = 7.8$ Hz, 2H), 7.45 (d, $J = 7.8$ Hz, 2H), 6.92 (m, 1H), 4.08 (m, 2H), 1.40 (s, 9H); MS (DCI/NH₃) m/z 223 (M + H)⁺.

6-[N-(4-(tert-Butoxycarbonylaminoethyl)phenyl)carbamyl]-2-naphthalenecarbonitrile (24) was prepared from **23** using the procedure described for the preparation of **14a**: ¹H NMR (DMSO-*d*₆) δ 10.68 (s, 1H), 8.70 (s, 1H), 8.58 (s, 1H), 8.33 (d, $J = 8.5$ Hz, 1H), 8.23 (d, $J = 7.8$ Hz, 1H), 8.18 (dd, $J = 7.8, 1.7$ Hz, 1H), 8.02 (dd, $J = 8.5, 1.7$ Hz, 1H), 7.88 (d, $J = 8.5$ Hz, 2H), 7.45 (d, $J = 8.5$ Hz, 2H), 4.08 (m, 2H), 1.48 (s, 9H); MS (DCI/NH₃) m/z 419 (M + NH₄)⁺.

6-[N-(4-(Aminomethyl)phenyl)carbamyl]-2-naphthalenecarboxamide (25) was prepared from **24** using the procedure described for the preparation of **6**. The crude product was purified by HPLC to provide **25**: ¹H NMR (DMSO-*d*₆) δ 10.68 (s, 1H), 9.52 (s, 2H), 9.39 (s, 2H), 8.71 (s, 1H), 8.57 (s, 1H), 8.32 (d, $J = 8.8$ Hz, 1H), 8.24 (d, $J = 8.8$ Hz, 1H), 8.20 (m, 3H), 8.17 (dd, $J = 8.5, 1.7$ Hz, 1H), 7.92 (dd, $J = 8.8, 2.1$ Hz, 1H), 7.87 (d, $J = 8.6$ Hz, 2H), 7.48 (d, $J = 8.6$ Hz, 2H), 4.08 (m, 2H); MS (DCI/NH₃) m/z 319 (M + H)⁺. Anal. (C₁₉H₁₈N₄O·2C₂HF₃O₂) C, H, N.

(4-tert-Butyldimethylsilyloxymethyl)aniline (26b). A solution of 4-aminobenzyl alcohol **26a** (1 g, 8.1 mmol) in DMF (20 mL) was treated with imidazole (0.54 g, 8.1 mmol) and TBSCl (1.22 g, 8.12 mmol); stirred overnight at room temperature; diluted with EtOAc (100 mL); washed with 1 M H₃PO₄, saturated NaHCO₃, and brine; dried (Na₂SO₄); filtered; and concentrated to an oil which was flash chromatographed on silica gel eluting with 25% EtOAc/hexanes to provide 0.5 g (26%) of **26b** as a clear oil: ¹H NMR (CDCl₃) δ 7.11 (d, $J = 8.3$ Hz, 2H), 6.66 (d, $J = 8.3$ Hz, 2H), 4.62 (s, 2H), 3.61 (bs, 2H), 0.93 (s, 9H), 0.07 (s, 6H); MS (DCI/NH₃) m/z 238 (M + H)⁺.

6-[N-(4-(Hydroxymethyl)phenyl)carbamyl]-2-naphthalenecarbonitrile (27). The TBS-protected amide was prepared from **26** (300 mg, 1.26 mmol) using the procedure described for the preparation of **14a**, and the crude product was carried on directly to the deprotection step: MS (DCI/NH₃) m/z 434 (M + NH₄)⁺.

The silyl ether in TBAF solution (1 M in THF, 2 mL) was stirred for 1 h, quenched with 10% NH₄Cl solution (50 mL), and diluted with EtOAc (100 mL). The layers were separated, and the organic layer was washed with brine, dried (MgSO₄), filtered, and concentrated to provide a light brown oil which was triturated with CH₂Cl₂ and filtered to provide 100 mg (26%) of **27** as a white solid: ¹H NMR (DMSO-*d*₆) δ 10.51 (s, 1 H), 8.68 (s, 1 H), 8.67 (s, 1H), 8.34 (d, $J = 8.5$ Hz, 1H), 8.23 (d, $J = 7.8$ Hz, 1H), 8.18 (d, $J = 7.8$ Hz, 1H), 7.95 (d, $J = 8.5$ Hz, 1H), 7.77 (d, $J = 8.5$ Hz, 2H), 7.33 (d, $J = 8.5$ Hz, 2H), 4.49 (d, 2 H), 3.08 (bs, 1H); MS (DCI/NH₃) m/z 320 (M + NH₄)⁺.

6-[N-(4-(Hydroxymethyl)phenyl)carbamyl]-2-naphthalenecarboxamide (28) was prepared from **27** using the procedure described for the preparation of **18**. The resulting brown solid was purified by HPLC to yield **28**: ¹H NMR (DMSO-*d*₆) δ 10.91 (s, 1H), 9.75 (br s, 4H), 8.93 (s, 1H), 8.79 (s, 1H), 8.53 (d, $J = 8.8$ Hz, 1H), 8.47 (m, 1H), 8.45 (d, $J = 8.8$ Hz, 1H), 8.38 (d, $J = 8.5$ Hz, 1H), 8.14 (d, $J = 8.5$ Hz, 1H), 8.08 (d, $J = 8.6$ Hz, 2H), 7.69 (d, $J = 8.6$ Hz, 2H), 4.25 (s, 2H); MS (DCI/NH₃) m/z 320 (M + H)⁺. Anal. (C₁₉H₁₇N₃O₂·C₂HF₃O₂) C, H, N.

6-[N-(4-Ethylphenyl)carbamyl]-2-naphthalenecarbonitrile (30a) was prepared from **29a** using the procedure described for the preparation of **14a**: ¹H NMR (CDCl₃) δ 10.44 (s, 1H), 8.73 (s, 1H), 8.63 (s, 1H), 8.29 (d, $J = 8.6$ Hz, 1H), 8.21 (d, $J = 8.6$ Hz, 1H), 8.08 (m, 2H), 7.72 (d, $J = 8.6$ Hz, 2H), 7.22 (d, $J = 8.6$ Hz, 2H), 2.60 (q, $J = 7.6$ Hz, 2H), 1.19 (t, $J = 7.6$ Hz, 3H); MS (DCI/NH₃) m/z 301 (M + H)⁺.

6-[N-(4-Ethylphenyl)carbamyl]-2-naphthalenecarboxamide (31a) was prepared from **30a** using the procedure

described for the preparation of **22**. The crude product was converted to the AcOH salt to provide pure **31a**: $^1\text{H NMR}$ (DMSO- d_6) δ 10.43 (br s, 1H), 8.63 (s, 1H), 8.47 (d, $J = 1.7$ Hz, 1H), 8.23–8.08 (m, 3H), 7.94 (dd, $J = 8.8$, 1.7 Hz, 1H), 7.72 (d, $J = 8.5$ Hz, 2H), 7.22 (d, $J = 8.5$ Hz, 2H), 2.60 (q, $J = 7.4$ Hz, 2H), 1.19 (t, $J = 7.4$ Hz, 3H); MS (ESI) m/z 318 (M + H) $^+$. Anal. (C₂₀H₁₉N₃O·C₂H₄O₂·0.5H₂O) C, H, N.

6-[N-(4-Carbamylphenyl)carbamyl]-2-naphthalenecarbonitrile (30b) was prepared from **29b** using the procedure described for the preparation of **33d**: $^1\text{H NMR}$ (DMSO- d_6) δ 10.73 (br s, 1H), 8.70 (s, 2H), 8.32 (s, 1H), 8.30 (d, $J = 8.8$ Hz, 1H), 8.23 (d, $J = 8.8$ Hz, 1H), 8.15 (dd, $J = 8.5$, 1.7 Hz, 1H), 7.92–7.87 (m, 5H), 7.27 (m, 1H); MS (DCI/NH₃) m/z 333 (M + NH₄) $^+$.

6-[N-(4-Carbamylphenyl)carbamyl]-2-naphthalenecarboxamidide (31b) was prepared from **30b** using the procedure described for the preparation of **18**. The crude product was purified by HPLC to provide **31b**: $^1\text{H NMR}$ (DMSO- d_6) δ 10.76 (s, 1H), 9.51 (s, 2H), 9.14 (s, 2H), 8.74 (s, 1H), 8.56 (s, 1H), 8.33 (d, $J = 8.8$ Hz, 1H), 8.26 (d, $J = 8.8$ Hz, 1H), 8.16 (dd, $J = 8.5$, 1.1 Hz, 1H), 7.91 (m, 6H), 7.31 (s, 1H); MS (DCI/NH₃) m/z 333 (M + H) $^+$. Anal. (C₁₉H₁₆N₄O₂·C₂HF₃O₂·1.25H₂O) C, H, N.

6-[N-(3-Methoxyphenyl)carbamyl]-2-naphthalenecarbonitrile (33a) was prepared from **32a** using the procedure described for the preparation of **33d**: $^1\text{H NMR}$ (DMSO- d_6) δ 10.51 (s, 1H), 8.68 (s, 1H), 8.66 (s, 1H), 8.29 (d, $J = 8.5$ Hz, 1H), 8.21 (d, $J = 8.9$ Hz, 1H), 8.14 (dd, $J = 8.5$, 1.6 Hz, 1H), 7.90 (d, $J = 8.5$, 1.7 Hz, 1H), 7.51 (s, 1H), 7.42 (d, $J = 8.9$ Hz, 1H), 7.29 (t, $J = 8.1$ Hz, 1H), 6.62 (d, $J = 8.1$ Hz, 1H), 3.78 (s, 3H); MS (APCI) m/z 303 (M + H) $^+$.

6-[N-(3-Methoxyphenyl)carbamyl]-2-naphthalenecarboxamidide (34a) was prepared from **33a** using the procedure described for the preparation of **6**. The crude product was purified by HPLC to provide **34a**: $^1\text{H NMR}$ (DMSO- d_6) δ 10.52 (s, 1H), 9.50 (s, 2H), 9.21 (s, 2H), 8.68 (s, 1H), 8.55 (s, 1H), 8.32 (d, $J = 8.9$ Hz, 1H), 8.23 (d, $J = 8.5$ Hz, 1H), 8.15 (dd, $J = 8.5$, 1.7 Hz, 1H), 7.91 (dd, $J = 8.5$, 1.7 Hz, 1H), 7.51 (s, 1H), 7.42 (d, $J = 8.8$ Hz, 1H), 7.29 (t, $J = 8.1$ Hz, 1H), 6.73 (dd, $J = 8.1$, 2.3 Hz, 1H), 3.78 (s, 3H); MS (APCI) m/z 320 (M + H) $^+$. Anal. (C₁₉H₁₇N₃O₂·C₂HF₃O₂·0.25H₂O) C, H, N.

6-[N-(3-Ethoxyphenyl)carbamyl]-2-naphthalenecarbonitrile (33b) was prepared from **32b** using the procedure described for the preparation of **33d**: $^1\text{H NMR}$ (DMSO- d_6) δ 10.51 (s, 1H), 8.68 (s, 1H), 8.66 (s, 1H), 8.29 (d, $J = 8.8$ Hz, 1H), 8.21 (d, $J = 8.8$ Hz, 1H), 8.14 (dd, $J = 8.5$, 1.7 Hz, 1H), 7.90 (d, $J = 8.5$, 1.7 Hz, 1H), 7.50 (s, 1H), 7.39 (m, 1H), 7.27 (t, $J = 8.0$ Hz, 1H), 6.70 (d, $J = 8.0$ Hz, 1H), 4.04 (q, $J = 7.0$ Hz, 2H), 1.35 (t, $J = 7.0$ Hz, 3H); MS (APCI) m/z 317 (M + H) $^+$.

6-[N-(3-Ethoxyphenyl)carbamyl]-2-naphthalenecarboxamidide (34b) was prepared from **33b** using the procedure described for the preparation of **6**. The crude product was purified by HPLC to provide **34b**: $^1\text{H NMR}$ (DMSO- d_6) δ 10.52 (s, 1H), 9.51 (s, 2H), 9.24 (s, 2H), 8.68 (s, 1H), 8.56 (s, 1H), 8.32 (d, $J = 8.9$ Hz, 1H), 8.24 (d, $J = 8.8$ Hz, 1H), 8.15 (dd, $J = 8.8$, 1.7 Hz, 1H), 7.90 (dd, $J = 8.5$, 1.7 Hz, 1H), 7.51 (s, 1H), 7.40 (d, $J = 9.1$ Hz, 1H), 7.27 (t, $J = 8.1$ Hz, 1H), 6.71 (dd, $J = 8.2$, 1.7 Hz, 1H), 4.04 (q, $J = 6.9$ Hz, 2H), 1.36 (t, $J = 6.9$ Hz, 3H); MS (APCI) m/z (M + H) $^+$ 334; HRMS (FAB) calcd 334.1556, found 334.1557. Anal. (C₂₀H₁₉N₃O₂·C₂HF₃O₂) C, H, N; calcd, 9.39; found, 9.82.

6-[N-(3-Isopropoxyphenyl)carbamyl]-2-naphthalenecarbonitrile (33c) was prepared from **32c** using the procedure described for the preparation of **33d**: $^1\text{H NMR}$ (CDCl₃) δ 9.74 (s, 1H), 8.59 (s, 1H), 8.32 (s, 1H), 8.17 (d, $J = 8.5$, 1.7 Hz, 1H), 8.09 (d, $J = 8.5$ Hz, 1H), 8.01 (d, $J = 8.5$ Hz, 1H), 7.69 (d, $J = 8.5$, 1.7 Hz, 1H), 7.55 (s, 1H), 7.26 (m, 2H), 6.69 (d, $J = 7.8$ Hz, 1H), 4.49 (sep, $J = 6.0$ Hz, 1H), 1.31 (d, $J = 6.0$ Hz, 6H); MS (APCI) m/z 331 (M + H) $^+$.

6-[N-(3-Isopropoxyphenyl)carbamyl]-2-naphthalenecarboxamidide (34c) was prepared from **33c** using the procedure described for the preparation of **6**. The crude product was purified by HPLC to provide **34c**: $^1\text{H NMR}$ (DMSO- d_6) δ

10.49 (s, 1H), 9.51 (s, 2H), 9.23 (s, 2H), 8.67 (s, 1H), 8.55 (s, 1H), 8.32 (d, $J = 8.5$ Hz, 1H), 8.23 (d, $J = 8.5$ Hz, 1H), 8.15 (dd, $J = 8.5$, 1.7 Hz, 1H), 7.89 (dd, $J = 8.5$, 1.7 Hz, 1H), 7.49 (s, 1H), 7.38 (d, $J = 8.8$ Hz, 1H), 7.26 (t, $J = 8.1$ Hz, 1H), 6.69 (dd, $J = 8.1$, 2.0 Hz, 1H), 4.59 (sep, $J = 6.3$ Hz, 1H), 1.30 (d, $J = 6.3$ Hz, 6H); MS (APCI) m/z 348 (M + H) $^+$. Anal. (C₂₁H₂₁N₃O₂·C₂HF₃O₂·0.75H₂O) C, H, N.

3-(3-Pentyloxy)aniline (32e), 3-Aminophenol **32d** (1.0 g, 9.2 mmol), PPh₃ (2.88 g, 11 mmol), and 3-pentanol (1.15 mL, 11 mmol) were dissolved in THF (25 mL). DEAD (1.91 g, 11 mmol) was then added dropwise over 1 min. The solution was allowed to stir for 15 min and was poured slowly into hexanes while the reaction stirred. Filtration through silica gel/Celite afforded 1.48 g (90%) of **32e** as a viscous yellow oil: $^1\text{H NMR}$ (CDCl₃) δ 7.03 (t, $J = 8.2$ Hz, 1H), 6.31 (m, 1H), 6.27 (m, 1H), 6.26 (s, 1H), 4.07 (p, 1H), 3.9–3.4 (br s, 2H), 1.64 (m, 4H), 0.94 (t, $J = 7.4$ Hz, 6H); MS (APCI) m/z 180 (M + H) $^+$.

3-Cyclopentylloxylaniline (32f) was prepared from **32d** using the procedure described for the preparation of **32e**: $^1\text{H NMR}$ (CDCl₃) δ 7.03 (t, $J = 7.8$ Hz, 1H), 6.32–6.22 (m, 3H), 4.71 (m, 1H), 3.9–3.4 (br s, 2H), 1.84 (m, 6H), 1.79 (m, 2H); MS (APCI) m/z 178 (M + H) $^+$.

6-[N-(3-(1-Ethylpropoxy)phenyl)carbamyl]-2-naphthalenecarbonitrile (33d). Compound **32e** (269 mg, 1.5 mmol), **12** (215 mg, 1 mmol), Et₃N (50 μL , 0.36 mmol), and DMAP (7 mg, 0.05 mmol) in CH₂Cl₂ (8 mL) were stirred for 18 h, concentrated, and flash chromatographed on silica gel eluting with 30% EtOAc/hexane to provide 263 mg (74%) of **33d** as a clear oil: $^1\text{H NMR}$ (CDCl₃) δ 9.59 (s, 1H), 8.41 (s, 1H), 8.29 (d, $J = 8.8$ Hz, 1H), 8.02 (m, 2H), 7.99 (br s, 1H), 7.70 (dd, $J = 8.5$, 1.7 Hz, 1H), 7.46 (t, $J = 2.0$ Hz, 1H), 7.26 (d, $J = 7.8$ Hz, 1H), 7.27 (d, $J = 6.1$ Hz, 1H), 7.13 (d, $J = 7.8$ Hz, 1H), 6.75 (d, $J = 7.8$ Hz, 1H), 4.19 (m, 1H), 1.70 (m, 4H), 0.96 (t, $J = 7.4$ Hz, 6H); MS (DCI/NH₃) m/z 359 (M + H) $^+$.

6-[N-(3-(1-Ethylpropoxy)phenyl)carbamyl]-2-naphthalenecarboxamidide (34d) was prepared from **33d** using the procedure described for the preparation of **6**. The crude product was purified by HPLC to provide **34d**: $^1\text{H NMR}$ (DMSO- d_6) δ 10.47 (s, 1H), 9.49 (s, 2H), 9.14 (s, 2H), 8.67 (s, 1H), 8.55 (s, 1H), 8.32 (d, $J = 8.8$ Hz, 1H), 8.24 (d, $J = 8.8$ Hz, 1H), 8.14 (dd, $J = 8.5$, 1.7 Hz, 1H), 7.90 (dd, $J = 8.5$, 1.7 Hz, 1H), 7.51 (s, 1H), 7.38 (d, $J = 8.8$ Hz, 1H), 7.26 (t, $J = 8.1$ Hz, 1H), 6.72 (dd, $J = 8.1$, 1.7 Hz, 1H), 4.19 (p, $J = 7.4$ Hz, 1H), 1.65 (m, 4H), 0.93 (t, $J = 7.4$ Hz, 6H); MS (DCI/NH₃) m/z 376 (M + H) $^+$. Anal. (C₂₃H₂₅N₃O₂·C₂HF₃O₂) C, H, N.

6-[N-(3-Cyclopentylloxyphenyl)carbamyl]-2-naphthalenecarbonitrile (33e) was prepared from **32f** using the procedure described for the preparation of **33d**: $^1\text{H NMR}$ (CDCl₃) δ 9.59 (s, 1H), 8.56 (s, 1H), 8.30 (s, 1H), 8.17 (d, $J = 8.8$, 1.7 Hz, 1H), 8.07 (d, $J = 8.5$ Hz, 1H), 7.98 (d, $J = 8.5$ Hz, 1H), 7.69 (dd, $J = 8.5$, 1.7 Hz, 1H), 7.54 (s, 1H), 7.26 (m, 2H), 6.67 (d, $J = 7.4$ Hz, 1H), 4.55 (sep, $J = 7.1$ Hz, 1H), 2.02–1.72 (m, 6H), 1.63 (m, 2H); MS (APCI) m/z 357 (M + H) $^+$.

6-[N-(3-Cyclopentylloxyphenyl)carbamyl]-2-naphthalenecarboxamidide (34e) was prepared from **33e** using the procedure described for the preparation of **6**. The crude product was purified by HPLC to provide **34e**: $^1\text{H NMR}$ (DMSO- d_6) δ 10.50 (s, 1H), 9.51 (s, 2H), 9.30 (s, 2H), 8.68 (s, 1H), 8.56 (s, 1H), 8.32 (d, $J = 8.8$ Hz, 1H), 8.24 (d, $J = 8.5$ Hz, 1H), 8.15 (dd, $J = 8.5$, 1.7 Hz, 1H), 7.90 (dd, $J = 8.5$, 1.7 Hz, 1H), 7.49 (s, 1H), 7.38 (d, $J = 8.1$ Hz, 1H), 7.25 (t, $J = 8.1$ Hz, 1H), 6.71 (dd, $J = 8.2$, 1.7 Hz, 1H), 4.04 (p, $J = 7.4$ Hz, 1H), 1.96–1.08 (m, 8H); MS (APCI) m/z 374 (M + H) $^+$. Anal. (C₂₃H₂₃N₃O₂·C₂HF₃O₂·0.25H₂O) C, H, N.

6-[N-(3-Phenoxyphenyl)carbamyl]-2-naphthalenecarbonitrile (33f) was prepared from **32g** using the procedure described for the preparation of **33d**: $^1\text{H NMR}$ (DMSO- d_6) δ 10.61 (s, 1H), 8.68 (s, 1H), 8.64 (s, 1H), 8.29 (d, $J = 8.8$ Hz, 1H), 8.20 (d, $J = 8.8$ Hz, 1H), 8.11 (dd, $J = 8.5$, 1.7 Hz, 1H), 7.90 (dd, $J = 8.4$, 1.7 Hz, 1H), 7.63 (d, $J = 8.8$ Hz, 1H), 7.56 (s, 1H), 7.41 (m, 3H), 7.17 (t, $J = 7.3$ Hz, 1H), 7.08 (d, $J = 7.4$, 2H), 6.81 (d, $J = 8.1$ Hz, 1H); MS (APCI) m/z 365 (M + H) $^+$.

6-[N-(3-Phenoxyphenyl)carbamyl]-2-naphthalenecarboxamidide (34f) was prepared from **33f** using the procedure

described for the preparation of **6**. The crude product was purified by HPLC to provide **34f**: $^1\text{H NMR}$ (DMSO- d_6) δ 10.62 (s, 1H), 9.50 (s, 2H), 9.20 (s, 2H), 8.66 (s, 1H), 8.55 (s, 1H), 8.30 (d, $J = 8.8$ Hz, 1H), 8.22 (d, $J = 8.8$ Hz, 1H), 8.16 (dd, $J = 8.5, 1.7$ Hz, 1H), 7.90 (dd, $J = 8.5, 1.7$ Hz, 1H), 7.63 (d, $J = 8.2$ Hz, 1H), 7.57 (s, 1H), 7.46–7.37 (m, 3H), 7.17 (t, $J = 7.3$ Hz, 1H), 7.07 (d, $J = 7.3$ Hz, 2H), 6.81 (dd, $J = 8.1, 2.1$ Hz, 1H); MS (APCI) m/z 382 (M + H) $^+$. Anal. (C₂₄H₁₉N₃O₂·C₂H₃F₃O₂) C, H, N.

3-(Cyclopentylmethyl)aniline (32h). Cyclopentyltriphenylphosphonium bromide (3.6 g, 8.75 mmol) was suspended in anhydrous THF (60 mL) and cooled to -78 °C. BuLi (3.5 mL, 8.75 mmol) was added dropwise over 10 min. After complete addition, the slurry was warmed to 0 °C, maintained at that temperature for 30 min, and then cooled to -78 °C. A solution of 3-nitrobenzaldehyde (1.06 g, 7 mmol) in THF (14 mL) was added to the above solution dropwise over 5 min, and the solution was allowed to warm to room temperature. The reaction was poured into ether and filtered through a plug of silica gel, concentrated, dissolved in ether, filtered through silica gel a second time, and concentrated to a clear oil. The crude olefin was dissolved in MeOH (10 mL) with AcOH (250 μL) and stirred with 10% Pd/C (100 mg) under 1 atm hydrogen for 18 h. The reaction was filtered through Celite and concentrated to afford 992 mg (81%) of **32i**: $^1\text{H NMR}$ (CDCl₃) δ 7.08 (t, $J = 8.6$ Hz, 1H), 6.63 (d, $J = 8.6$ Hz, 1H), 6.59 (s, 2H), 4.75–3.75 (br s, 2H), 2.52 (d, $J = 6.4$ Hz, 2H), 2.11 (m, 1H), 1.65 (m, 4H), 1.51 (m, 2H), 1.20 (m, 2H); MS (APCI) m/z 176 (M + H) $^+$.

6-[N-(3-(Cyclopentylmethyl)phenyl)carbamyl]-2-naphthalenecarbonitrile (33g) was prepared from **32h** using the procedure described for the preparation of **33d**: $^1\text{H NMR}$ (DMSO- d_6) δ 10.46 (s, 1H), 8.68 (s, 1H), 8.67 (s, 1H), 8.28 (d, $J = 8.4$ Hz, 1H), 8.20 (d, $J = 8.9$ Hz, 1H), 8.15 (dd, $J = 8.8, 1.7$ Hz, 1H), 7.90 (dd, $J = 8.4, 1.7$ Hz, 1H), 7.66 (m, 2H), 7.28 (t, $J = 8.1$ Hz, 1H), 6.96 (d, $J = 7.4$ Hz, 1H), 2.59 (d, $J = 6.6$ Hz, 2H), 2.12 (m, 1H), 1.65 (m, 4H), 1.53 (m, 2H), 1.21 (m, 2H); MS (APCI) m/z 355 (M + H) $^+$.

6-[N-(3-(Cyclopentylmethyl)phenyl)carbamyl]-2-naphthalenecarboxamidine (34g) was prepared from **33g** using the procedure described for the preparation of **6**. The crude product was purified by HPLC and converted to the HCl salt to give **34g**: $^1\text{H NMR}$ (DMSO- d_6) δ 10.48 (s, 1H), 9.55 (s, 2H), 9.18 (s, 2H), 8.70 (s, 1H), 8.56 (s, 1H), 8.31 (d, $J = 8.8$ Hz, 1H), 8.23 (d, $J = 8.9$ Hz, 1H), 8.17 (d, $J = 1.4$ Hz, 1H), 8.16 (d, $J = 1.7$ Hz, 1H), 7.91 (dd, $J = 8.5, 2.1$ Hz, 1H), 7.66 (m, 2H), 7.28 (t, $J = 7.5$ Hz, 1H), 6.97 (d, $J = 7.5$ Hz, 1H), 2.59 (d, $J = 7.1$ Hz, 2H), 2.10 (m, 1H), 1.74–1.55 (m, 4H), 1.51 (m, 2H), 1.21 (m, 2H); MS (APCI) m/z 372 (M + H) $^+$. Anal. (C₂₄H₂₅N₃O·HCl·H₂O) C, H, N.

6-[N-(3,5-Dimethoxyphenyl)carbamyl]-2-naphthalenecarbonitrile (36a) was prepared from 3,5-dimethoxyaniline **35a** using the procedure described for the preparation of **33d**: $^1\text{H NMR}$ (CDCl₃) δ 8.42 (s, 1H), 8.30 (s, 1H), 8.06 (d, $J = 9$ Hz, 1H), 8.05 (s, 2H), 7.90 (br s, 1H), 7.72 (d, $J = 9$ Hz, 1H), 6.94 (d, $J = 2.1$ Hz, 2H), 6.32 (t, $J = 2.1$ Hz, 1H); MS (DCI/NH₃) m/z 333 (M + H) $^+$.

6-[N-(3,5-Dimethoxyphenyl)carbamyl]-2-naphthalenecarboxamidine (37a) was prepared from **36a** using the procedure described for the preparation of **6**. The crude product was converted to the CH₃SO₃H salt to provide pure **37a**: $^1\text{H NMR}$ (DMSO- d_6) δ 10.50 (s, 1H), 9.51 (s, 2H), 9.14 (s, 2H), 8.68 (s, 1H), 8.56 (s, 1H), 8.33 (d, $J = 8.9$ Hz, 1H), 8.24 (d, $J = 8.9$ Hz, 1H), 8.14 (dd, $J = 8.5, 1.7$ Hz, 1H), 7.90 (dd, $J = 8.5, 1.6$ Hz, 1H), 7.13 (d, $J = 2.1$ Hz, 2H), 6.31 (t, $J = 2.1$ Hz, 1H), 3.76 (s, 6H), 2.33 (s, 3.75H); MS (DCI/NH₃) m/z 350 (M + H) $^+$. Anal. (C₂₀H₁₉N₃O₃·1.25CH₄SO₃·H₂O) C, H, N.

3-Amino-5-methoxyphenol (35b). To a solution of **35a** (61.2 g, 400 mmol) in NMP (300 mL) was added NaOMe (56.0 g, 800 mmol) and the reaction was heated to 140 °C for 1 h. The reaction was cooled, poured into saturated NaH₂PO₄ solution (500 mL), and extracted with EtOAc (3 × 300 mL). The extracts were washed with brine, dried (Na₂SO₄), filtered, and condensed. The crude product was flash chromatographed

on silica gel eluting with 50% EtOAc/hexanes to yield 30.7 g (55%) of **35b**: $^1\text{H NMR}$ (DMSO- d_6) δ 8.86 (s, 1H), 5.61 (m, 2H), 5.53 (dd, $J = 2.4, 2.4$ Hz, 1H), 4.91 (br s, 2H), 3.58 (s, 3H); MS (DCI/NH₃) m/z 140 (M + NH₄) $^+$.

3-Isopropoxy-5-methoxyaniline (35c) was prepared from **35b** using the procedure described for the preparation of **32e**: $^1\text{H NMR}$ (CDCl₃) δ 5.92 (dd, $J = 2.5, 2.5$ Hz, 1H), 5.87 (m, 2H), 4.47 (sep, $J = 7.1$ Hz, 1H), 4.0–3.5 (br s, 2H), 3.74 (s, 3H), 1.31 (d, $J = 7.1$ Hz, 6H); MS (DCI/NH₃) m/z 182 (M + NH₄) $^+$.

3-Amino-5-isopropoxyphenol (35d) was prepared from **35c** using the procedure described for the preparation of **35b**: $^1\text{H NMR}$ (DMSO- d_6) δ 8.80 (s, 1H), 5.59 (m, 2H), 5.50 (dd, $J = 2.2, 2.2$ Hz, 1H), 4.85 (br s, 2H), 4.34 (sep, $J = 7.2$ Hz, 1H), 1.19 (d, $J = 7.2$ Hz, 6H); MS (DCI/NH₃) m/z 168 (M + NH₄) $^+$.

3,5-Diisopropoxyaniline (35e) was prepared from **35d** using the procedure described for the preparation of **32e**: $^1\text{H NMR}$ (CDCl₃) δ 5.90 (t, $J = 2.5$ Hz, 1H), 5.84 (d, $J = 2.5$ Hz, 2H), 4.45 (sep, $J = 7.0$ Hz, 2H), 3.85–3.55 (br s, 2H), 1.30 (d, $J = 7.0$ Hz, 12H); MS (DCI/NH₃) m/z 210 (M + NH₄) $^+$.

3-Cyclopentyl-5-isopropoxyaniline (35f) was prepared from **35d** using the procedure described for the preparation of **32e**: $^1\text{H NMR}$ (CDCl₃) δ 5.90 (dd, $J = 2.5, 2.7$ Hz, 1H), 5.86 (m, 2H), 4.68 (m, 1H), 4.46 (sep, $J = 7.0$ Hz, 1H), 4.10–3.85 (br s, 2H), 1.90–1.72 (m, 6H), 1.59 (m, 2H), 1.31 (d, $J = 7.0$ Hz, 6H); MS (DCI/NH₃) m/z 236 (M + NH₄) $^+$.

6-[N-(3,5-Diisopropoxyphenyl)carbamyl]-2-naphthalenecarbonitrile (36b) was prepared from **35e** using the procedure described for the preparation of **33d**: $^1\text{H NMR}$ (CDCl₃) δ 8.49 (s, 1H), 8.38 (s, 1H), 8.04 (d, $J = 8.9$ Hz, 1H), 8.01 (s, 2H), 7.89 (br s, 1H), 7.69 (dd, $J = 8.9, 1.7$ Hz, 1H), 6.89 (d, $J = 2.1$ Hz, 2H), 6.29 (t, $J = 2.1$ Hz, 1H), 4.55 (sep, $J = 7.1$ Hz, 2H), 1.34 (d, $J = 7.1$ Hz, 12H); MS (DCI/NH₃) m/z 389 (M + H) $^+$.

6-[N-(3,5-Diisopropoxyphenyl)carbamyl]-2-naphthalenecarboxamidine (37b) was prepared from **36b** using the procedure described for the preparation of **6**. The crude product was converted to the CH₃SO₃H salt to provide pure **37b**: $^1\text{H NMR}$ (DMSO- d_6) δ 10.40 (s, 1H), 9.49 (s, 2H), 9.11 (s, 2H), 8.66 (s, 1H), 8.55 (s, 1H), 8.32 (d, $J = 8.9$ Hz, 1H), 8.23 (d, $J = 8.5$ Hz, 1H), 8.12 (dd, $J = 8.5, 1.7$ Hz, 1H), 7.90 (dd, $J = 8.9, 1.7$ Hz, 1H), 7.07 (d, $J = 2.2$ Hz, 2H), 6.22 (t, $J = 2.2$ Hz, 1H), 4.55 (sep, $J = 7.0$ Hz, 2H), 2.31 (s, 6.75H), 1.29 (d, $J = 7.0$ Hz, 12H); MS (DCI/NH₃) m/z 406 (M + H) $^+$. Anal. (C₂₄H₂₇N₃O₃·2.25CH₄SO₃·0.5H₂O) C, H, N.

6-[N-(3-Cyclopentyl-5-isopropoxyphenyl)carbamyl]-2-naphthalenecarbonitrile (36c) was prepared from **35f** using the procedure described for the preparation of **33d**: $^1\text{H NMR}$ (CDCl₃) δ 8.49 (s, 1H), 8.39 (s, 1H), 8.05 (d, $J = 8.9$ Hz, 1H), 8.01 (s, 2H), 7.85 (br s, 1H), 7.70 (dd, $J = 8.6, 1.8$ Hz, 1H), 6.88 (m, 2H), 6.28 (t, $J = 2.0$ Hz, 1H), 4.77 (m, 1H), 4.55 (sep, $J = 7.0$ Hz, 1H), 1.95–1.72 (m, 6H), 1.52 (m, 2H), 1.34 (d, $J = 7.0$ Hz, 6H); MS (DCI/NH₃) m/z 415 (M + H) $^+$.

6-[N-(3-Cyclopentyl-5-isopropoxyphenyl)carbamyl]-2-naphthalenecarboxamidine (37c) was prepared from **36c** using the procedure described for the preparation of **6**. The crude product was converted to the CH₃SO₃H salt to provide pure **37c**: $^1\text{H NMR}$ (DMSO- d_6) δ 10.40 (s, 1H), 9.49 (s, 2H), 9.12 (s, 2H), 8.66 (s, 1H), 8.55 (s, 1H), 8.32 (d, $J = 8.9$ Hz, 1H), 8.23 (d, $J = 8.6$ Hz, 1H), 8.12 (dd, $J = 8.6, 1.7$ Hz, 1H), 7.90 (dd, $J = 8.9, 1.7$ Hz, 1H), 7.07 (d, $J = 2.1$ Hz, 2H), 6.21 (t, $J = 2.1$ Hz, 1H), 4.76 (m, 1H), 4.55 (sep, $J = 7.2$ Hz, 1H), 2.31 (s, 3.75H), 1.92 (m, 2H), 1.71 (m, 4H), 1.60 (m, 2H), 1.29 (d, $J = 7.2$ Hz, 6H); MS (DCI/NH₃) m/z 432 (M + H) $^+$. Anal. (C₂₆H₂₉N₃O₃·1.25CH₄SO₃·0.25H₂O) C, H, N.

1-Isopropyl-7-nitro-3,4-dihydroisoquinoline (40a). A solution of **39a**³² (730 mg, 4.2 mmol) in concentrated H₂SO₄ (7.5 mL) was stirred at 0 °C as KNO₃ (0.47 g, 4.6 mmol) was added. The reaction mixture was stirred at 0 °C for 30 min, then ice and water were added. The mixture was basicified at 0 °C with 25% NaOH and was then extracted with CH₂Cl₂ (3 × 200 mL). The organic layer was washed with water and brine, dried (MgSO₄), filtered, condensed, and flash chromatographed on silica gel eluting with 30% EtOAc/hexanes to afford

560 mg (61%) of **40a** as a yellow oil: $^1\text{H NMR}$ (CDCl_3) δ 8.38 (d, $J = 2.2$ Hz, 1H), 8.22 (dd, $J = 8.5, 2.2$ Hz, 1H), 7.39 (d, $J = 8.5$ Hz, 1H), 3.74 (t, $J = 7.2$ Hz, 2H), 3.32 (m, 1H), 2.77 (t, $J = 7.2$ Hz, 2H), 1.24 (d, $J = 6.6$ Hz, 6H); MS (DCI/ NH_3) m/z 219 ($\text{M} + \text{H}$) $^+$.

1-Isopropyl-7-amino-3,4-dihydroisoquinoline (41a). Compound **40a** (180 mg, 0.82 mmol) was hydrogenated in a Parr shaker at 4 atm for 48 h with Raney nickel (0.12 g) in EtOAc (30 mL). The reaction mixture was degassed, filtered through Celite, and evaporated to afford 155 mg (100%) of **41a**: $^1\text{H NMR}$ (CDCl_3) δ 6.99 (d, $J = 8.0$ Hz, 1H), 6.88 (d, $J = 2.2$ Hz, 1H), 6.70 (dd, $J = 8.0, 2.2$ Hz, 1H), 3.63 (t, $J = 7.3$ Hz, 2H), 3.20 (sep, $J = 6.8$ Hz, 1H), 2.54 (t, $J = 7.3$ Hz, 2H), 1.20 (d, $J = 6.8$ Hz, 6H); MS (DCI/ NH_3) m/z 189 ($\text{M} + \text{H}$) $^+$.

6-[N-(1-Isopropyl-3,4-dihydro-7-isoquinolinyl)carbamyl]-2-naphthalenecarbonitrile (42a) was prepared from **41a** using the procedure described for the preparation of **33d**: $^1\text{H NMR}$ ($\text{DMSO}-d_6$) δ 10.86 (s, 1H), 8.71 (s, 2H), 8.56 (s, 1H), 8.32 (d, $J = 8.7$ Hz, 1H), 8.25 (d, $J = 8.7$ Hz, 1H), 8.18 (dd, $J = 8.5, 1.8$ Hz, 1H), 8.14 (dd, $J = 8.5, 1.8$ Hz, 1H), 7.94 (dd, $J = 8.5, 1.1$ Hz, 1H), 7.57 (dd, $J = 8.5, 1.1$ Hz, 1H), 3.85 (t, $J = 7.4$ Hz, 2H), 3.61 (sep, $J = 6.6$ Hz, 1H), 3.07 (t, $J = 7.4$ Hz, 2H), 1.39 (d, $J = 6.6$ Hz, 6H); MS (DCI/ NH_3) m/z 368 ($\text{M} + \text{H}$) $^+$.

6-[N-(1-Isopropyl-3,4-dihydro-7-isoquinolinyl)carbamyl]-2-naphthalenecarboxamidine (43a) was prepared from **42a** using the procedure described for the preparation of **6**. The crude product was purified by HPLC to provide **43a**: $^1\text{H NMR}$ ($\text{DMSO}-d_6$) δ 10.88 (s, 1H), 9.52 (s, 2H), 9.26 (s, 2H), 8.75 (s, 1H), 8.57 (s, 1H), 8.54 (s, 1H), 8.34 (d, $J = 8.8$ Hz, 1H), 8.27 (d, $J = 8.5$ Hz, 1H), 8.19 (dd, $J = 8.5, 1.7$ Hz, 1H), 8.14 (d, $J = 8.8$ Hz, 1H), 7.94 (dd, $J = 8.3, 1.7$ Hz, 1H), 7.55 (d, $J = 8.3$ Hz, 1H), 3.84 (t, $J = 8.14$ Hz, 2H), 3.60 (sep, $J = 6.8$ Hz, 1H), 3.04 (t, $J = 8.14$ Hz, 2H), 1.38 (d, $J = 6.8$ Hz, 6H); MS (DCI/ NH_3) m/z 385 ($\text{M} + \text{H}$) $^+$. Anal. ($\text{C}_{24}\text{H}_{24}\text{N}_4\text{O}\cdot 2\text{C}_2\text{HF}_3\text{O}_2\cdot 1.25\text{H}_2\text{O}$) C, H, N.

7-Amino-1-isopropyl-1,2,3,4-tetrahydroisoquinoline (44a). NaBH_4 (200 mg, 5.3 mmol) was added portionwise to a 0 °C solution of **41a** (210 mg, 1.1 mmol) in MeOH (10 mL). The reaction mixture was refluxed for 30 min and then was cooled to 0 °C, and acetone (5 mL) was added dropwise. The solvent was evaporated and water (25 mL) was added to the residue. The mixture was extracted with ether (3 \times 30 mL). The organic layer was washed with brine, dried (MgSO_4), filtered, and evaporated to afford 200 mg (96%) of **44a**: $^1\text{H NMR}$ (CDCl_3) δ 6.87 (d, $J = 8.5$ Hz, 1H), 6.51 (m, 2H), 3.86 (d, $J = 3.4$ Hz, 1H), 3.51 (s, 2H), 3.27 (m, 1H), 2.88 (m, 1H), 2.72 (m, 1H), 2.56 (m, 1H), 2.29 (m, 1H), 1.61 (s, 1H), 1.11 (d, $J = 7.1$ Hz, 3H), 0.75 (d, $J = 6.8, 3\text{H}$); MS (DCI/ NH_3) m/z 191 ($\text{M} + \text{H}$) $^+$.

7-Amino-2-tert-butoxycarbonyl-1-isopropyl-1,2,3,4-tetrahydroisoquinoline (45a). Di-*tert*-butyl dicarbonate (250 mg, 1.15 mmol) was added to a 0 °C solution of **44a** (200 mg, 1.05 mmol) in CH_2Cl_2 (5 mL). The reaction mixture was stirred for 2 h at 0 °C, then water (20 mL) was added. The mixture was extracted with CH_2Cl_2 (3 \times 20 mL). The extracts were washed with 5% citric acid, saturated NaHCO_3 , and brine; dried (MgSO_4); filtered; and evaporated to afford 250 mg (82%) of **45a** as a colorless oil: $^1\text{H NMR}$ (CDCl_3) δ 7.03 (t, $J = 6.8$ Hz, 0.5H), 6.92 (t, $J = 7.5$ Hz, 0.5H), 6.59–6.40 (m, 3H), 4.80–4.58 (m, 1H), 3.98 (m, 0.5H), 3.69 (m, 0.5H), 3.47 (m, 0.5H), 3.35 (m, 0.5H), 2.76 (m, 2H), 1.97 (m, 1H), 1.46 (d, $J = 4.4$ Hz, 9H), 0.97 (m, 6H); MS (DCI/ NH_3) m/z 291 ($\text{M} + \text{H}$) $^+$.

6-[N-(2-tert-butoxycarbonyl-1-isopropyl-1,2,3,4-tetrahydro-7-isoquinolinyl)carbamyl]-2-naphthalenecarbonitrile (46a) was prepared from **45a** using the procedure described for the preparation of **33d**: $^1\text{H NMR}$ (CDCl_3) δ 8.43 (s, 1H), 8.30 (s, 1H), 8.04 (t, $J = 8.5$ Hz, 3H), 7.94 (s, 1H), 7.67 (m, 2H), 7.35 (d, $J = 7.5$ Hz, 1H), 4.81 (m, 1H), 4.05 (s, 0.5H), 3.81 (s, 0.5H), 3.50 (s, 0.5H), 3.38 (s, 1H), 2.86 (s, 2H), 2.06 (s, 1H), 1.48 (s, 9H), 1.02 (m, 6H); MS (ESI) m/z 468 ($\text{M} - 1$) $^-$.

6-[N-(1-Isopropyl-1,2,3,4-tetrahydro-7-isoquinolinyl)carbamyl]-2-naphthalenecarboxamidine (47a) was pre-

pared from **46a** using the procedure described for the preparation of **6**. The crude product was purified by HPLC to provide **47a**: $^1\text{H NMR}$ ($\text{DMSO}-d_6$) δ 10.61 (s, 1H), 9.50 (s, 2H), 9.35 (s, 1H), 9.22 (s, 2H), 8.69 (s, 1H), 8.56 (s, 1H), 8.34 (s, 1H), 8.32 (d, $J = 8.8$ Hz, 1H), 8.25 (d, $J = 8.8$ Hz, 1H), 8.24 (d, $J = 8.8$ Hz, 1H), 8.16 (dd, $J = 8.5, 1.7$ Hz, 1H), 7.91 (dd, $J = 8.5, 2.0$ Hz, 1H), 7.83 (d, $J = 1.7$ Hz, 1H), 7.70 (dd, $J = 8.5, 2.0$ Hz, 1H), 7.28 (d, $J = 8.5$ Hz, 1H), 4.49 (s, 1H), 3.27 (s, 2H), 2.98 (m, 2H), 2.42 (m, 1H), 1.11 (d, $J = 6.8$ Hz, 3H), 0.93 (d, $J = 6.8$ Hz, 3H); MS (DCI/ NH_3) m/z 387 ($\text{M} + \text{H}$) $^+$. Anal. ($\text{C}_{24}\text{H}_{26}\text{N}_4\text{O}\cdot 3\text{C}_2\text{HF}_3\text{O}_2$) C, H, N.

7-Nitro-1-(2-methylpropyl)-3,4-dihydroisoquinoline (40b) was prepared from **39b** using the procedure described for the preparation of **40a**: $^1\text{H NMR}$ (CDCl_3) δ 8.32 (d, $J = 2.3$ Hz, 1H), 8.22 (dd, $J = 8.1, 2.3$ Hz, 1H), 7.38 (d, $J = 8.1$ Hz, 1H), 3.74 (t, $J = 5.9$ Hz, 2H), 2.79 (m, 2H), 2.68 (d, $J = 5.9$ Hz, 2H), 2.08–2.11 (m, 1H), 0.98 (d, $J = 6.4$ Hz, 6H); MS (DCI/ NH_3) m/z 233 ($\text{M} + \text{H}$) $^+$.

7-Amino-1-(2-methylpropyl)-3,4-dihydroisoquinoline (41b) was prepared from **40b** using the procedure described for the preparation of **41a**: $^1\text{H NMR}$ (CDCl_3) δ 6.99 (d, $J = 8.1$ Hz, 1H), 6.81 (d, $J = 2.2$ Hz, 1H), 6.69 (dd, $J = 8.1, 2.2$ Hz, 1H), 3.62 (m, 4H), 2.56 (t, $J = 4.7$ Hz, 2H), 2.07 (m, 1H), 0.94 (d, $J = 6.8$ Hz, 6H); MS (DCI/ NH_3) m/z 203 ($\text{M} + \text{H}$) $^+$.

6-[N-(1-(2-Methylpropyl)-3,4-dihydro-7-isoquinolinyl)carbamyl]-2-naphthalenecarbonitrile (42b) was prepared from **41b** using the procedure described for the preparation of **33d**: $^1\text{H NMR}$ ($\text{DMSO}-d_6$) δ 10.84 (s, 1H), 8.71 (d, $J = 1.8$ Hz, 2H), 8.45 (d, $J = 1.1$ Hz, 1H), 8.33 (d, $J = 8.5$ Hz, 1H), 8.25 (d, $J = 8.5$ Hz, 1H), 8.18 (dd, $J = 8.5, 1.1$ Hz, 1H), 8.12 (dd, $J = 8.5, 1.8$ Hz, 1H), 7.93 (dd, $J = 8.5, 1.1$ Hz, 1H), 7.56 (d, $J = 8.5$ Hz, 1H), 3.87 (t, $J = 7.4$ Hz, 2H), 3.07 (t, $J = 7.7$ Hz, 2H), 2.93 (d, $J = 7.4$ Hz, 2H), 2.13 (m, 1H), 0.99 (d, $J = 6.3$ Hz, 6H); MS (DCI/ NH_3) m/z 382 ($\text{M} + \text{H}$) $^+$.

6-[N-(1-(2-Methylpropyl)-3,4-dihydro-7-isoquinolinyl)carbamyl]-2-naphthalenecarboxamidine (43b) was prepared from **42b** using the procedure described for the preparation of **6**. The crude product was purified by HPLC to provide **43b**: $^1\text{H NMR}$ ($\text{DMSO}-d_6$) δ 10.91 (s, 1H), 9.51 (s, 2H), 9.28 (s, 2H), 8.74 (s, 1H), 8.57 (s, 1H), 8.49 (d, $J = 1.7$ Hz, 1H), 8.35 (d, $J = 8.8$ Hz, 1H), 8.27 (d, $J = 8.5$ Hz, 1H), 8.20 (dd, $J = 8.5, 1.7$ Hz, 1H), 8.18 (d, $J = 8.8$ Hz, 1H), 7.92 (dd, $J = 8.5, 1.7$ Hz, 1H), 7.58 (d, $J = 8.5$ Hz, 1H), 3.93 (t, $J = 8.0$ Hz, 2H), 3.11 (t, $J = 8.0$ Hz, 2H), 2.97 (d, $J = 6.5$ Hz, 2H), 2.14 (m, 1H), 1.00 (d, $J = 6.8$ Hz, 6H); MS (ESI) m/z 399 ($\text{M} + \text{H}$) $^+$. Anal. ($\text{C}_{25}\text{H}_{26}\text{N}_4\text{O}\cdot 2\text{C}_2\text{HF}_3\text{O}_2\cdot 1.5\text{H}_2\text{O}$) C, H, N.

7-Amino-1-(2-methylpropyl)-1,2,3,4-tetrahydroisoquinoline (44b) was prepared from **41b** using the procedure described for the preparation of **44a**: $^1\text{H NMR}$ (CDCl_3) δ 6.87 (d, $J = 8.1$ Hz, 1H), 6.50 (dd, $J = 8.1, 2.4$ Hz, 1H), 6.45 (d, $J = 2.4$ Hz, 1H), 3.91 (m, 1H), 3.52 (s, 2H), 3.19 (m, 1H), 2.94 (m, 1H), 2.67 (m, 2H), 1.86 (m, 2H), 1.67 (m, 1H), 1.52 (m, 1H), 1.01 (d, $J = 6.6$ Hz, 3H), 0.97 (d, $J = 6.6$ Hz, 3H); MS (DCI/ NH_3) m/z 205 ($\text{M} + \text{H}$) $^+$.

7-Amino-2-tert-butoxycarbonyl-1-(2-methylpropyl)-1,2,3,4-tetrahydroisoquinoline (45b) was prepared from **44b** using the procedure described for the preparation of **45a**: $^1\text{H NMR}$ (CDCl_3) δ 6.97 (m, 2H), 6.67 (m, 1H), 6.57 (s, 1H), 4.17 (m, 1H), 3.14 (m, 1H), 2.83 (m, 1H), 2.60 (m, 1H), 1.72 (m, 4H), 1.49 (s, 9H), 1.05 (d, $J = 6.6$ Hz, 3H), 0.93 (d, $J = 6.6$ Hz, 3H); MS (DCI/ NH_3) m/z 305 ($\text{M} + \text{H}$) $^+$.

6-[N-(2-tert-butoxycarbonyl-1-(2-methylpropyl)-1,2,3,4-tetrahydro-7-isoquinolinyl)carbamyl]-2-naphthalenecarbonitrile (46b) was prepared from **45b** using the procedure described for the preparation of **33d**: $^1\text{H NMR}$ (CDCl_3) δ 8.43 (s, 1H), 8.30 (s, 1H), 8.03 (m, 3H), 7.95 (s, 1H), 7.71 (dd, $J = 8.5, 1.0$ Hz, 1H), 7.54 (m, 1H), 7.33 (m, 1H), 7.12 (m, 1H), 4.22 (m, 1H), 4.07 (m, 1H), 3.20 (m, 1H), 2.93 (m, 1H), 2.70 (m, 1H), 1.82 (m, 1H), 1.70 (m, 1H), 1.50 (s, 9H), 1.26 (t, $J = 7.1$ Hz, 1H), 1.08 (d, $J = 6.1$ Hz, 3H), 0.96 (d, $J = 6.4$ Hz, 3H); MS (ESI) m/z 482 ($\text{M} - 1$) $^-$.

6-[N-(1-(2-Methylpropyl)-1,2,3,4-tetrahydro-7-isoquinolinyl)carbamyl]-2-naphthalenecarboxamidine (47b) was prepared from **46b** using the procedure described for the

preparation of **6**. The crude product was purified by HPLC to provide **47b**: $^1\text{H NMR}$ (DMSO- d_6) δ 10.53 (s, 1H), 9.51 (s, 2H), 9.26 (s, 2H), 8.82 (s, 1H), 8.70 (s, 1H), 8.56 (s, 1H), 8.33 (d, J = 8.8 Hz, 1H), 8.25 (d, J = 8.8 Hz, 1H), 8.16 (dd, J = 8.5, 1.1 Hz, 1H), 7.91 (dd, J = 8.5, 1.5 Hz, 1H), 7.74 (d, J = 7.4 Hz, 2H), 7.27 (d, J = 8.8 Hz, 1H), 4.55 (s, 1H), 3.35 (m, 2H), 3.00 (m, 2H), 1.81 (m, 3H), 1.03 (d, J = 6.6 Hz, 6H); MS (DCI/NH₃) m/z 401 (M + H)⁺. Anal. (C₂₅H₂₈N₄O·2.5C₂H₅F₃O₂) C, H, N.

N-(2-Phenylethyl)cyclopentanecarboxamide (38b). Phenethylamine **38a** (4.5 mL, 35.8 mmol) was added dropwise to a 0 °C suspension of cyclopentanecarboxylic acid (3.9 mL, 35.8 mmol), EDCI (13.7 g, 71.7 mmol), DMAP (8.6 g, 71.7 mmol), and THF (130 mL). The reaction mixture was stirred for 30 min at 0 °C and for 15 h at room temperature. Water (100 mL) was added and the mixture was extracted with EtOAc (3 × 100 mL). The combined extracts were washed with saturated NaHCO₃, 1 M HCl, water, and brine; dried (MgSO₄); filtered; and evaporated. The crude product was purified by flash chromatography on silica gel eluting with 30% EtOAc/hexanes to afford 7.45 g (94%) of **38b** as a white solid: $^1\text{H NMR}$ (CDCl₃) δ 7.35–7.14 (m, 6H), 3.52 (dt, J = 6.8, 6.1 Hz, 2H), 2.42 (t, J = 6.8 Hz, 2H), 2.44 (m, 1H), 1.86–1.62 (m, 8H), 1.61–1.46 (m, 2H); MS (DCI/NH₃) m/z 218 (M + H)⁺.

1-Cyclopentyl-3,4-dihydroisoquinoline (39c). This preparation follows the procedure of Larsen et al.³³ (COCl)₂ (2.2 mL, 36 mmol) was added dropwise to a 0 °C solution of **38b** (7.08 g, 32.6 mmol) and CH₂Cl₂ (335 mL). The reaction mixture was stirred for 15 min at 0 °C and for 30 min at room temperature. After cooling to –15 °C, FeCl₃ (6.4 g, 39 mmol) was added in portions. The reaction mixture was stirred for 15 min at –15 °C and then was allowed to warm to room-temperature overnight. After cooling to 0 °C, 2 M HCl (275 mL) was added slowly, and the solution was stirred for 1 h at room temperature. The layers were separated and the aqueous layer was extracted with CH₂Cl₂ (2 × 200 mL). The combined organic layers were washed with brine, dried (MgSO₄), filtered, and evaporated to afford an orange oil. The oil was dissolved in MeOH (200 mL), H₂SO₄ (13 mL) was added slowly, and the reaction mixture was refluxed for 15 h. Solvent was evaporated, and water (100 mL) was added. The solution was washed with EtOAc (3 × 100 mL), and the washes were discarded. The aqueous layer was cooled to 0 °C and was basicified with 28% NH₄OH. The basic solution was extracted with CH₂Cl₂ (3 × 100 mL). The basic extracts were combined, washed with brine, dried (MgSO₄), filtered, and evaporated to afford 3.9 g (60%) of **39c** as a brown oil: $^1\text{H NMR}$ (CDCl₃) δ 7.55 (m, 1H), 7.34–7.17 (m, 3H), 3.67 (t, J = 7.5 Hz, 2H), 3.37 (m, 1H), 2.66 (t, J = 7.5 Hz, 2H), 2.02–1.58 (m, 8H); MS (DCI/NH₃) m/z 200 (M + H)⁺.

7-Nitro-1-cyclopentyl-3,4-dihydroisoquinoline (40c) was prepared from **39c** using the procedure described for the preparation of **40a**: $^1\text{H NMR}$ (CDCl₃) δ 8.38 (d, J = 2.4 Hz, 1H), 8.21 (dd, J = 8.2, 2.4 Hz, 1H), 7.37 (d, J = 8.2 Hz, 1H), 3.74 (t, J = 7.4 Hz, 2H), 3.41 (m, 1H), 2.77 (d, J = 7.4 Hz, 2H), 2.06–1.89 (m, 2H), 1.89–1.62 (m, 6H); MS (DCI/NH₃) m/z 245 (M + H)⁺.

7-Amino-1-cyclopentyl-3,4-dihydroisoquinoline (41c) was prepared from **40c** using the procedure described for the preparation of **41a**: $^1\text{H NMR}$ (CDCl₃) δ 6.97 (d, J = 8.1 Hz, 1H), 6.88 (d, J = 2.3 Hz, 1H), 6.68 (dd, J = 8.1, 2.3 Hz, 1H), 3.63 (m, 4H), 3.29 (m, 1H), 2.53 (t, J = 7.3 Hz, 2H), 1.91 (m, 2H), 1.77 (m, 4H), 1.63 (m, 2H); MS (DCI/NH₃) m/z 215 (M + H)⁺.

6-[N-(1-Cyclopentyl-3,4-dihydro-7-isoquinolinyl)carbamyl]-2-naphthalenecarbonitrile (42c) was prepared from **41c** using the procedure described for the preparation of **33d**: $^1\text{H NMR}$ (DMSO- d_6) δ 10.62 (s, 1H), 8.70 (br s, 2H), 8.31 (d, J = 8.9 Hz, 1H), 8.23 (d, J = 8.8 Hz, 1H), 8.16 (dd, J = 8.8, 1.5 Hz, 1H), 8.08 (s, 1H), 7.92 (dd, J = 8.4, 1.5 Hz, 1H), 7.87 (dd, J = 8.1, 1.9 Hz, 1H), 7.27 (d, J = 8.1 Hz, 1H), 3.57 (t, J = 7.2 Hz, 2H), 3.34 (m, 1H), 2.59 (d, J = 7.2 Hz, 2H), 1.92 (m, 2H), 1.78 (m, 2H), 1.64 (m, 4H); MS (DCI/NH₃) m/z 394 (M + H)⁺.

6-[N-(1-Cyclopentyl-3,4-dihydro-7-isoquinolinyl)carbamyl]-2-naphthalenecarboxamide (43c) was prepared

from **42c** using the procedure described for the preparation of **6**. The crude product was purified by HPLC and converted to the HCl salt to provide **43c**: $^1\text{H NMR}$ (DMSO- d_6) δ 10.88, (s, 1H), 9.52 (s, 2H), 9.26 (s, 2H), 8.75 (s, 1H), 8.57 (s, 1H), 8.54 (s, 1H), 8.34 (d, J = 8.8 Hz, 1H), 8.27 (d, J = 8.5 Hz, 1H), 8.19 (dd, J = 8.5, 1.4 Hz, 1H), 8.14 (d, J = 8.8 Hz, 1H), 7.94 (dd, J = 8.3, 2.0 Hz, 1H), 7.55 (d, J = 8.3 Hz, 1H), 3.84 (t, J = 8.1 Hz, 2H), 3.60 (m, 1H), 3.04 (m, 2H), 1.38 (d, J = 6.8 Hz, 6H); MS (ESI) m/z 411 (M + H)⁺. Anal. (C₂₆H₂₆N₄O·4HCl) C, H, N.

7-Amino-1-cyclopentyl-1,2,3,4-tetrahydroisoquinoline (44c) was prepared from **41c** using the procedure described for the preparation of **44a**: $^1\text{H NMR}$ (CDCl₃) δ 6.86 (d, J = 8.1 Hz, 1H), 6.52 (m, 2H), 3.82 (d, J = 6.5 Hz, 1H), 3.50 (m, 3H), 3.23 (m, 1H), 2.93 (m, 1H), 2.68 (m, 2H), 2.39 (m, 1H), 1.82–1.41 (m, 6H), 1.31 (m, 2H); MS (DCI/NH₃) m/z 217 (M + H)⁺.

7-Amino-2-tert-butoxycarbonyl-1-cyclopentyl-1,2,3,4-tetrahydroisoquinoline (45c) was prepared from **44c** using the procedure described for the preparation of **45a**: $^1\text{H NMR}$ (CDCl₃) δ 6.91 (d, J = 7.0 Hz, 1H), 6.53 (m, 2H), 4.86 (d, J = 9.9 Hz, 0.5H), 4.70 (d, J = 9.2 Hz, 0.5H), 4.05 (m, 0.5H), 3.80 (m, 0.5H), 3.75 (br s, 3H), 3.42 (m, 0.5H), 3.30 (m, 0.5H), 2.75 (m, 2H), 2.14 (m, 1H), 1.77–1.55 (m, 6H), 1.51 (m, 2H), 1.45 (s, 9H); MS (DCI/NH₃) m/z 317 (M + H)⁺.

6-[N-(2-tert-Butoxycarbonyl-1-cyclopentyl-1,2,3,4-tetrahydro-7-isoquinolinyl)carbamyl]-2-naphthalenecarbonitrile (46c) was prepared from **45c** using the procedure described for the preparation of **33d**: $^1\text{H NMR}$ (CDCl₃) δ 8.44 (s, 1H), 8.29 (s, 1H), 8.03 (m, 4H), 7.71 (m, 2H), 7.34 (m, 1H), 7.15 (d, J = 8.4 Hz, 1H), 4.98 (d, J = 9.6 Hz, 0.5H), 4.86 (d, J = 9.2 Hz, 0.5H), 4.12 (m, 0.5H), 3.91 (m, 0.5H), 3.50–3.28 (m, 1H), 2.87 (m, 2H), 2.18 (m, 1H), 1.71 (m, 4H), 1.48 (s, 9H), 1.47 (m, 4H); MS (ESI) m/z 496 (M + H)⁺.

6-[N-(1-Cyclopentyl-1,2,3,4-dihydro-7-isoquinolinyl)carbamyl]-2-naphthalenecarboxamide (47c) was prepared from **46c** using the procedure described for the preparation of **6**. The crude product was purified by HPLC and converted to the HCl salt to provide **47c**: $^1\text{H NMR}$ (DMSO- d_6) δ 10.69 (s, 1H), 9.72 (s, 2H), 9.61 (s, 2H), 9.34 (s, 2H), 8.75 (s, 1H), 8.60 (s, 1H), 8.32 (d, J = 8.8 Hz, 1H), 8.24 (d, J = 8.5 Hz, 1H), 8.18 (dd, J = 8.5, 1.4 Hz, 1H), 7.93 (dd, J = 8.5, 1.7 Hz, 1H), 7.85 (d, J = 1.7 Hz, 1H), 7.74 (dd, J = 8.1, 1.7 Hz, 1H), 7.25 (d, J = 8.5 Hz, 1H), 4.42 (m, 1H), 3.42 (m, 2H), 3.05 (m, 2H), 2.41 (m, 1H), 1.80 (m, 2H), 1.70 (s, 2H), 1.52 (m, 4H); MS (ESI) m/z 413 (M + H)⁺. Anal. (C₂₆H₂₈N₄O·2HCl·1.5H₂O) C, H, N.

2-(2-Ethoxycarbonyl-5-nitrophenyl)-2-ethylmalonic Acid, Dimethyl Ester (49). To a solution of **48**³⁴ (16.0 g, 53.8 mmol) in acetone (450 mL) was added K₂CO₃ (22.0 g, 159 mmol) followed by EtI (20.0 mL, 292 mmol) and the mixture was refluxed for 14 h. The solvent was evaporated, EtOAc (200 mL) was added, and the mixture was washed with water (3 × 100 mL) and brine, dried (MgSO₄), filtered, and evaporated to afford 18.6 g (98%) of **49** as light reddish oil: $^1\text{H NMR}$ (CDCl₃) δ 8.24 (m, 2H), 8.11 (d, J = 8.1 Hz, 1H), 4.33 (m, 2H), 3.72 (s, 6H), 2.58 (q, J = 7.5 Hz, 2H), 1.38 (t, J = 7.2 Hz, 3H), 0.98 (t, J = 7.5 Hz, 3H); MS (ESI) m/z 354 (M + H)⁺.

2-(2-Carboxy-5-nitrophenyl)butanoic Acid (50). To a suspension of **49** (22.0 g, 62.3 mmol) in a mixture of water (300 mL) and EtOH (100 mL) was added 50% aqueous NaOH (30 mL), and the mixture was heated to reflux for 2.5 h. The reaction was cooled, acidified with 6 M HCl, refluxed for 30 min, and then cooled. The product, which precipitated upon cooling, was filtered, washed with water, and dried under vacuum to afford 3.9 g (78%) of **50** as a pale yellow solid: $^1\text{H NMR}$ (DMSO- d_6) δ 8.20 (m, 2H), 8.00 (d, J = 8.5 Hz, 1H), 4.38 (t, J = 7.4 Hz, 1H), 1.93 (m, 2H), 0.84 (t, J = 7.4 Hz, 3H); MS (ESI) m/z 252 (M – 1)⁺.

2-(2-Hydroxymethyl-5-nitrophenyl)-1-butanol (51a). To a solution of **50** (11.25 g, 44.4 mmol) in THF (100 mL) at room temperature was added a solution of 1 M BH₃ in THF (133 mL) and the mixture was allowed to stir overnight. The reaction mixture was quenched with 1 M citric acid, the solvent was partially concentrated, and EtOAc (150 mL) was added.

The mixture was washed with water (60 mL), 1 M NaOH (60 mL), water, and brine; dried (MgSO₄); filtered; and evaporated to afford 9.2 g (92%) of **51a** as a light yellow oil: ¹H NMR (CDCl₃) δ 8.15 (d, *J* = 2.3 Hz, 1H), 8.09 (dd, *J* = 8.5, 2.3 Hz, 1H), 7.53 (d, *J* = 8.5 Hz, 1H), 4.91 (d, *J* = 12.4 Hz, 1H), 4.59 (d, *J* = 12.4 Hz, 1H), 3.98 (dd, *J* = 10.0, 6.0 Hz, 1H), 3.67 (dd, *J* = 10.0, 4.6 Hz, 1H), 3.20 (m, 1H), 1.73 (m, 2H), 0.84 (t, *J* = 7.3 Hz, 3H); MS (DCI/NH₃) *m/z* 243 (M + NH₄)⁺.

N-Allyl-4-ethyl-6-nitro-1,2,3,4-tetrahydroisoquinoline (52a). To a solution of **51a** (6.13 g, 27.2 mmol) in THF (80 mL) at 0 °C were added TEA (12.0 mL, 86.1 mmol) and DMAP (30 mg, 0.24 mmol), followed by MsCl (4.85 mL, 61.2 mmol). After 15 min, allylamine (4.7 g, 81.6 mmol) was added and the mixture was stirred at 0 °C for 15 min, room temperature for 12 h, and finally 75 °C for 4 h. The reaction mixture was cooled, EtOAc (120 mL) and water (70 mL) were added, and the organic phase was washed with water (2 × 50 mL) and brine, dried (MgSO₄), filtered, and evaporated. The product was flash chromatographed on silica gel eluting with 15% EtOAc/hexanes to afford 4.50 g (67%) of **52a** as a light yellow oil: ¹H NMR (CDCl₃) δ 8.09 (d, *J* = 2.4 Hz, 1H), 7.96 (dd, *J* = 8.5, 2.4 Hz, 1H), 7.15 (d, *J* = 8.5 Hz, 1H), 5.91 (m, 1H), 5.26 (m, 2H), 3.66 (m, 2H), 3.18 (m, 2H), 2.86 (m, 1H), 2.69 (m, 2H), 1.80 (m, 2H), 1.00 (t, *J* = 7.5 Hz, 3H); MS (ESI) *m/z* 247 (M + H)⁺.

N-Allyl-6-amino-4-ethyl-1,2,3,4-tetrahydroisoquinoline (53a). To a solution of **52a** (1.00 g, 4.1 mmol) in CH₂Cl₂ (10 mL) were successively added water (1 mL), 1,1'-di-*n*-octyl-4,4'-bipyridinium dibromide (10 mg, 18.4 μmol), and a solution of K₂CO₃ (2.80 g, 20.3 mmol) and Na₂S₂O₄ (3.18 g, 18.3 mmol) in water (10 mL). A very strong blue color developed and the mixture was heated at 35 °C for 24 h, at which time the color had dissipated. An additional solution of K₂CO₃ (500 mg, 3.62 mmol) and Na₂S₂O₄ (500 mg, 2.88 mmol) in water (2 mL) was added to the reaction and the resulting mixture was stirred for an additional 1 h. Water (30 mL) was added to the mixture and the aqueous layer was extracted with CH₂Cl₂ (3 × 40 mL). The combined CH₂Cl₂ layers were dried (MgSO₄) and filtered through a plug of silica gel, eluting with 5% MeOH/EtOAc to afford 694 mg (79%) of **53a** as a white solid: ¹H NMR (CDCl₃) δ 6.81 (d, *J* = 8.1 Hz, 1H), 6.55 (d, *J* = 2.2 Hz, 1H), 6.49 (dd, *J* = 8.1, 2.2 Hz, 1H), 5.92 (m, 1H), 5.20 (m, 2H), 3.49 (m, 2H), 3.12 (m, 2H), 2.26 (m, 3H), 1.71 (m, 2H), 0.96 (t, *J* = 7.4 Hz, 3H); MS (ESI) *m/z* 217 (M + H)⁺.

6-[N-(4-Ethyl-1,2,3,4-tetrahydro-2-(2-propenyl)-6-isoquinolinyl)carbonyl]-2-naphthalenecarbonitrile (54a) was prepared from **53a** using the procedure described for the preparation of **33d**: ¹H NMR (CDCl₃) δ 10.42 (s, 1H), 8.44 (s, 1H), 8.27 (s, 1H), 8.05 (m, 3H), 7.69 (dd, *J* = 8.5, 1.7 Hz, 1H), 7.62 (s, 1H), 7.41 (d, *J* = 8.1 Hz, 1H), 7.04 (d, *J* = 8.1 Hz, 1H), 5.96 (m, 1H), 5.28 (m, 2H), 3.61 (m, 2H), 3.19 (m, 2H), 2.70 (m, 3H), 1.80 (m, 2H), 0.99 (t, *J* = 7.5 Hz, 3H); MS (ESI) *m/z* 396 (M + H)⁺.

6-[N-(4-Ethyl-1,2,3,4-tetrahydro-2-(2-propenyl)-6-isoquinolinyl)carbonyl]-2-naphthalenecarboxamide (55a) was prepared from **54a** using the procedure described for the preparation of **6**: ¹H NMR (DMSO-*d*₆) δ 10.60 (s, 1H), 10.10 (br. s, 1H), 9.52 (s, 2H), 9.16 (s, 2H), 8.70 (s, 1H), 8.57 (s, 1H), 8.34–8.14 (m, 3H), 7.90 (m, 2H), 7.74 (m, 1H), 7.27 (d, *J* = 8.5 Hz, 1H), 6.02 (m, 1H), 5.63 (m, 2H), 4.37 (m, 2H), 3.78 (m, 2H), 3.33–3.09 (m, 2H), 2.08–1.74 (m, 2H), 0.91 (t, *J* = 8.7 Hz, 3H); MS (ESI) *m/z* 413 (M + H)⁺.

6-[N-(4-Ethyl-1,2,3,4-tetrahydro-6-isoquinolinyl)carbonyl]-2-naphthalenecarboxamide (56a). To a solution of Pd(dba)₂ (17.1 mg, 0.018 mmol) in THF (3 mL) was added DPPB (7.9 mg, 0.018 mmol) and the mixture was stirred for 20 min. Thiosalicylic acid (87 mg, 0.56 mmol) was added and the resulting mixture was transferred via cannula to a solution of **55a** (154 mg, 0.37 mmol) in DMF (3 mL). After 2.5 h the reaction mixture was quenched with 1 M HCl and diluted with water (20 mL) and EtOAc (20 mL). The aqueous phase was separated, concentrated, and purified by HPLC to yield 115 mg (48%) of **56a** as a white powder: ¹H NMR (DMSO-*d*₆) δ 10.60 (s, 1H), 9.50 (s, 2H), 9.25 (s, 2H), 9.03 (br d, 2H), 8.70

(s, 1H), 8.56 (s, 1H), 8.33–8.17 (m, 3H), 7.88 (m, 2H), 7.72 (m, 1H), 7.25 (d, *J* = 9.5 Hz, 1H), 4.26 (br s, 2H), 3.25–3.03 (m, 4H), 1.92–1.71 (m, 2H), 0.98 (t, *J* = 8.5 Hz, 3H); MS (ESI) *m/z* 373 (M + H)⁺. Anal. (C₂₃H₂₄N₄O·2.25C₂HF₃O₂·1.5H₂O) C, H, N.

N-Allyl-6-nitro-1,2,3,4-tetrahydroisoquinoline (52b) was prepared from **51b**³⁴ as described in the procedure for preparation of **52a**: ¹H NMR (CDCl₃) δ 7.97 (m, 2H), 7.17 (d, *J* = 8.5 Hz, 1H), 5.93 (m, 1H), 5.27 (m, 2H), 3.70 (s, 2H), 3.20 (d, *J* = 6.8 Hz, 2H), 3.00 (t, *J* = 5.9 Hz, 2H), 2.78 (t, *J* = 5.9 Hz, 2H); MS (ESI) *m/z* 219 (M + H)⁺.

N-Allyl-6-amino-1,2,3,4-tetrahydroisoquinoline (53b) was prepared from **52b** using the procedure described for the preparation of **53a**: ¹H NMR (CDCl₃) δ 6.82 (d, *J* = 8.1 Hz, 1H), 6.48 (m, 2H), 5.94 (m, 1H), 5.26 (m, 2H), 3.57 (s, 2H), 3.19 (d, *J* = 6.6 Hz, 2H), 2.84 (t, *J* = 5.9 Hz, 2H), 2.74 (t, *J* = 5.9 Hz, 2H); MS (ESI) *m/z* 189 (M + H)⁺.

6-[N-(1,2,3,4-Tetrahydro-2-(2-propenyl)-6-isoquinolinyl)carbonyl]-2-naphthalenecarbonitrile (54b) was prepared from **53b** using the procedure described for the preparation of **33d**: ¹H NMR (CDCl₃) δ 10.43 (s, 1H), 8.67 (m, 2H), 8.33–8.12 (m, 3H), 7.88 (m, 1H), 7.56 (m, 2H), 7.05 (d, *J* = 8.5 Hz, 1H), 5.95–5.76 (m, 1H), 5.22 (m, 2H), 3.53 (s, 2H), 3.13 (d, *J* = 6.4 Hz, 2H), 2.83 (t, *J* = 5.8 Hz, 2H), 2.67 (t, *J* = 5.8 Hz, 2H); MS (ESI) *m/z* 368 (M + H)⁺.

6-[N-(1,2,3,4-Tetrahydro-2-(2-propenyl)-6-isoquinolinyl)carbonyl]-2-naphthalenecarboxamide (55b) was prepared from **54b** using the procedure described for the preparation of **6**: ¹H NMR (DMSO-*d*₆) δ 10.61 (s, 1H), 10.14 (s, 1H), 9.50 (s, 2H), 9.20 (s, 2H), 8.68 (s, 1H), 8.56 (s, 1H), 8.32 (d, *J* = 8.5 Hz, 1H), 8.24 (d, *J* = 8.5 Hz, 1H), 8.15 (dd, *J* = 8.5, 1.6 Hz, 1H), 7.91 (dd, *J* = 8.5, 1.6 Hz, 1H), 7.79 (s, 1H), 7.70 (m, 1H), 7.26 (d, *J* = 8.5 Hz, 1H), 6.00 (m, 1H), 5.60 (m, 2H), 4.37 (m, 2H), 3.81 (m, 2H), 3.15 (m, 2H); MS (ESI) *m/z* 385 (M + H)⁺.

6-[N-(1,2,3,4-Tetrahydro-6-isoquinolinyl)carbonyl]-2-naphthalenecarboxamide (56b) was prepared from **55b** using the procedure described for the preparation of **56a**. The crude product was purified by HPLC to provide **56a**: ¹H NMR (DMSO-*d*₆) δ 10.55 (s, 1H), 9.48 (s, 2H), 9.12 (s, 2H), 8.97 (br s, 1H), 8.68 (s, 1H), 8.55 (s, 1H), 8.31 (d, *J* = 8.7 Hz, 1H), 8.23 (d, *J* = 8.7 Hz, 1H), 8.15 (dd, *J* = 8.7, 1.7 Hz, 1H), 7.90 (dd, *J* = 8.4, 2.0 Hz, 1H), 7.75 (s, 1H), 7.66 (dd, *J* = 8.4, 2.0 Hz, 1H), 7.24 (d, *J* = 8.4 Hz, 1H), 4.27 (s, 2H), 3.41 (t, *J* = 6.1 Hz, 2H), 3.03 (t, *J* = 6.1 Hz, 2H); MS (ESI) *m/z* 345 (M + H)⁺. Anal. (C₂₁H₂₀N₄O·2.25C₂HF₃O₂·1.5H₂O) C, H, N.

Enzymology. Synthetic compounds were tested in a spectrophotometric assay for their inhibitory activity toward urokinase and several other serine proteases, using chromogenic substrates (DiaPharma Group, Inc. Distributor of Chromogenix). Their inhibitory activity was determined from comparison of their reaction rates to the substrate alone. The assay was performed in a 96-well, polystyrene, flat-bottom plate in 50 mM Tris/0.15 M NaCl + 0.5% Pluronic F-68 (Sigma P-5556), pH 7.4 (with HCl) buffer. The compounds were dissolved in DMSO and tested at 0.01–250 μM concentration in a final reaction volume of 200 μL. The reactions were initiated by the addition of substrate and were followed by the formation of *p*-nitroaniline at 405 nm on the Spectromax (Molecular Devices) plate reader for 15 min. The Spectromax determined the reaction rates that were used to calculate percent inhibition. *K_i* values were calculated from the percent inhibition and previously established *K_m* values. Enzymes, substrates, and their concentrations in the assay: human uPA (Abbokinase, Abbott Laboratories, Abbott Park, IL), 2–3 nM; substrate, pyroGlu-Arg-pNA-HCl (S-2444), 200 μM; human plasma kallikrein (Sigma), 100 ng/mL; substrate, H-D-Pro-Phe-Arg-pNA-2HCl (S-2302), 330 μM; human plasmin (DiaPharma), 18 nM; substrate, H-D-Val-Leu-Lys-pNA-2HCl (S-2251), 360 μM; human alpha thrombin (Enzyme Research Laboratories), 8.2 nM; substrate, H-D-Pro-Phe-Arg-pNA-2HCl (S-2302), 820 μM; human tPA (Sigma), 1 μg/mL; substrate,

H-D-Ile-Pro-Arg-pNA-2HCl (S-2288), 1350 μ M; porcine trypsin (Sigma), 1.25 nM; substrate, pyroGlu-Arg-pNA-HCl (S-2444), 200 μ M.

Crystallography. Procedures for preparation of uPA-inhibitor complexes and data processing have been reported by Nienaber et al.⁴³ Resolution (in Å), temperature factors (*B*, in Å²), and PDB atomic coordinate codes for the structures referred to in the text are as follows: **6** (resolution 2.0, *B* 2.0–16.8, code 1OWE); **25** (1.6, 2.7–16.6, 1OWH); **34e** (2.9, 11.9–26.1, 1OWI); **43a** (3.1, 14, 1OWJ); **47a** (2.8, 17, 1OWK); **56a** (2.3, 23.6, 1OWD).

Supporting Information Available: NMR spectra of compounds **14**, **15**, and **34b**. This material is available free of charge via the Internet at <http://pubs.acs.org>.

References

- (1) (a) Cook, A. D.; Braine, E. L.; Campbell, I. K.; Hamilton, J. A. Differing roles for urokinase and tissue-type plasminogen activator in collagen-induced arthritis. *Am. J. Pathol.* **2002**, *160*, 917–926. (b) Busso, N.; Pleclat, V.; So, A.; Sappino, A.-P. Plasminogen activation in synovial tissues: Differences between normal, osteoarthritis, and rheumatoid arthritis joints. *Ann. Rheum. Dis.* **1997**, *56*, 550–557.
- (2) (a) Noda-Heiny, H.; Daugherty, A.; Sobel, B. E. Augmented urokinase receptor expression in atheroma. *Arterioscler. Thromb. Vasc. Biol.* **1995**, *15*, 37–43. (b) Carmeliet, P.; Moons, L.; Lijnen, R.; Baes, M.; Lemaitre, V.; Tipping, P.; Drew, A.; Eeckhout, Y.; Shapiro, S.; Lupu, F.; Collen, D. Urokinase-generated plasmin activates matrix metalloproteinases during aneurism formation. *Nature Genet.* **1997**, *17*, 439–444. (c) Falkenberg, M.; Giglio, D.; Bjornheden, T.; Nygren, H.; Risberg, B. Urokinase Plasminogen Activator Colocalizes with CD25+ Cells in Atherosclerotic Vessels. *J. Vasc. Res.* **1998**, *35*, 318–324. (d) Preissner, K. T.; Kanse, S. M.; Chavakis, T.; May, A. E.; The Dual Role of the Urokinase Receptor System in Pericellular Proteolysis and Cell Adhesion. Implications for Cardiovascular Function. *Basic. Res. Cardiol.* **1999**, *94*, 315–321.
- (3) Kanse, S. M.; Benzakour, O.; Kanthou, C.; Kost, C.; Lijnen, H. R.; Preissner, K. T. Induction of Vascular SMC Proliferation by Urokinase Indicates a Novel Mechanism of Action in Vasoproliferative Disorders. *Arterioscler. Thromb. Vasc. Biol.* **1997**, *17*, 2848–285.
- (4) (a) Rabbani, S. A.; Xing, R. H. Role of urokinase (uPA) and its receptor (uPAR) in invasion and metastasis of hormone-dependent malignancies. *J. Int. Oncol.* **1998**, *12*, 911–920. Bell, W. R. The fibrinolytic system in neoplasia. *Sem. Thromb. Hemost.* **1996**, *22*, 459–478. (b) Blasi, F. The Urokinase Receptor. A Cell Surface, Regulated Chemokine. *APMIS* **1999**, *107*, 96–101.
- (5) (a) Andreasen, P. A.; Kjoller, L.; Christensen, L.; Duffy, M. J. The Urokinase-type Plasminogen Activator System in Cancer Metastasis: A Review. *Int. J. Cancer* **1997**, *72*, 1–22. (b) Achbarou, A.; Kaiser, S.; Tremblay, G.; Sainte-Marie, L. G.; Brodt, P.; Goltzman, D.; Rabbani, S. A. *Cancer Res.* **1994**, *54*, 2372–2377. (c) Duffy, M. J. Urokinase-type plasminogen activator: a potent marker of metastatic potential in human cancers. *Biochem. Soc. Trans.* **2002**, *30*, 207–210.
- (6) Shapiro, R. L.; Duquette, J. G.; Roses, D. F.; Nunes, I.; Harris, M. N.; Kamino, H.; Wilson, E. L.; Rifkin, D. B. Induction of primary cutaneous melanocytic neoplasms in urokinase-type plasminogen activator (uPA)-deficient and wild-type mice: Cellular blue nevi invade but do not progress to malignant melanoma in uPA-deficient animals. *Cancer Res.* **1996**, *56*, 3597–3604.
- (7) Bugge, T. H.; Lund, L. R.; Kombrinck, K. K.; Nielsen, B. S.; Holmbäck, K.; Drew, A. F.; Flick, M. J.; Witte, D. P.; Danø, K.; Degen, J. L. Reduced metastasis of Polyoma virus middle T antigen-induced mammary cancer in plasminogen-deficient mice. *Oncogene* **1998**, *16*, 3097–3104.
- (8) Evans, D.; Sloan-Stakleff, K.; Arvan, M.; Guyton, D. Time and dose-dependency of the suppression of pulmonary metastasis of rat mammary cancer by amiloride. *Clin. Exp. Metastasis* **1998**, *16*, 353–357.
- (9) Rabbani, S.; Harakidas, P.; Davidson, D.; Henkin, J.; Mazar, A. Prevention of prostate-cancer metastasis in vivo by a novel synthetic inhibitor of urokinase-type plasminogen activator. *Int. J. Cancer* **1995**, *63*, 840–845.
- (10) Alonso, D. F.; Tejera, A. M.; Farias, E. F.; Bal de Kier Joffe, E.; Bomez, D. E. Inhibition of mammary tumor cell adhesion, migration, and invasion by the selective synthetic urokinase inhibitor B428. *Anticancer Res.* **1998**, *18*, 4499–4504.
- (11) Alonso, D. F.; Farias, E. F.; Ladeda, V.; Davel, L.; Puricelli, L.; Bal de Kier Joffe, E. Effects of synthetic urokinase inhibitors on local invasion and metastasis in a murine mammary tumor model. *Breast Cancer Res. Treat.* **1996**, *40*, 209–223.
- (12) Xing, R. H.; Mazar, A.; Henkin, J.; Rabbani, S. A. Prevention of breast cancer growth, invasion, and metastasis by antiestrogen tamoxifen alone or in combination with urokinase inhibitor B-428. *Cancer Res.* **1997**, *57*, 3585–3593.
- (13) Stürzebecher, J.; Markwardt, F. Synthetische Inhibitoren der Serineproteinasen. *Pharmazie* **1978**, *33*, 599–602.
- (14) Tidwell, R. R.; Geratz, J. D.; Dubovi, E. J. Aromatic amidines. Comparison of their ability to block respiratory syncytial virus induced cell fusion and to inhibit plasmin, urokinase, thrombin, and trypsin. *J. Med. Chem.* **1983**, *26*, 294–298.
- (15) (a) Yang, H.; Henkin, J. Selective Inhibition of Urokinase by Substituted Phenylguanidines: Quantitative Structure–Activity Relationship Analyses. *J. Med. Chem.* **1990**, *33*, 2956–2961. (b) Yang, H.; Henkin, J. Competitive Inhibitors of Human Urokinase. *Fibrinolysis* **1992**, *6* (Suppl. 1), 31–34.
- (16) Vassalli, J.-D.; Belin, D. Amiloride selectively inhibits the urokinase-type plasminogen activator. *FEBS Lett.* **1987**, *214*, 187–191.
- (17) Towle, M. J.; Lee, A.; Maduakor, E. C.; Schwartz, C. E.; Bridges, A. J.; Littlefield, B. A. Inhibition of urokinase by 4-substituted benzo[b]thiophene-2-carboxamidines: An important new class of selective synthetic urokinase inhibitor. *Cancer Res.* **1993**, *53*, 2553–2559.
- (18) Bridges, A. J.; Lee, A.; Schwartz, C. E.; Towle, M. J.; Littlefield, B. A. The synthesis of three 4-substituted benzo[b]thiophene-2-carboxamidines as potent and selective inhibitors of urokinase. *Bioorg. Med. Chem.* **1993**, *1*, 403–410.
- (19) Rudolph, M. J.; Illig, C. R.; Subasinghe, N. L.; Wilson, K. J.; Hoffman, J. B.; Randle, T.; Green, D.; Molloy, C. J.; Soll, R. M.; Lewandowski, F.; Zhang, M.; Bone, R.; Spurlino, J. C.; Deckman, I. C.; Manthey, C.; Sharp, C.; Maguire, D.; Grasperger, B. L.; DesJarlais, R. L.; Zhou, Z. Design and Synthesis of 4,5-Disubstituted-thiophene-2-amidines as Potent Urokinase Inhibitors. *Bioorg. Med. Chem. Lett.* **2002**, *12*, 491–495.
- (20) Stürzebecher, J.; Vieweg, H.; Steinmetzer, T.; Schweinitz, A.; Stubbs, M. T.; Renatus, M.; Wikström, P. 3-Amidinophenylalanine-based Inhibitors of Urokinase. *Bioorg. Med. Chem. Lett.* **1999**, *9*, 3147–3152.
- (21) Sperl, S.; Jacob, U.; Arroyo de Prada, N.; Stürzebecher, J.; Wilhelm, O. G.; Bode, W.; Magdolen, V.; Huber, R.; Moroder, L. (4-Aminomethyl)phenylguanidine Derivatives as Nonpeptidic Highly Selective Inhibitors of Human Urokinase. *Proc. Natl. Acad. Sci. U.S.A.* **2000**, *97*, 5113–5118.
- (22) (a) Barber, C. G.; Dickinson, R. P.; Horne, V. A. Selective Urokinase-Type Plasminogen Activator (uPA) Inhibitors. Part 1: 2-Pyridinylguanidines. *Bioorg. Med. Chem. Lett.* **2002**, *12*, 181–184. (b) Barber, C. G.; Dickinson, R. P. Selective Urokinase-Type Plasminogen Activator (uPA) Inhibitors. Part 2: (3-Substituted-5-halo-2-pyridinyl)guanidines. *Bioorg. Med. Chem. Lett.* **2002**, *12*, 185–187.
- (23) (a) Mackman, R. L.; Hui, H. C.; Breitenbucher, G.; Katz, B. A.; Luong, C.; Martelli, A.; McGee, D.; Radika, K.; Sendzik, M.; Spencer, J. R.; Sprengeler, P. A.; Tario, J.; Verner, E.; Wang, J. 2-(2-Hydroxy-3-alkoxyphenyl)-1H-benzimidazole-5-carboxamide Derivatives as Potent and Selective Urokinase-type Plasminogen Activator Inhibitors. *Bioorg. Med. Chem. Lett.* **2002**, *12*, 2019–2022. (b) Mackman, R. L.; Katz, B. A.; Breitenbucher, J. G.; Hui, H. C.; Verner, E.; Luong, C.; Liu, L.; Sprengeler, P. A. Exploiting Subsite S1 of Trypsin-Like Serine Proteases for Selectivity: Potent and Selective Inhibitors of Urokinase-Type Plasminogen Activator. *J. Med. Chem.* **2001**, *44*, 3856–3871. (c) Verner, E.; Katz, B. A.; Spencer, J. R.; Allen, D.; Hataya, J.; Hruzewicz, W.; Hui, H. C.; Kolesnikov, A.; Li, Y.; Luong, C.; Martelli, A.; Radika, K.; Rai, R.; She, M.; Shrader, W.; Sprengeler, P. A.; Trapp, S.; Wang, J.; Young, W. B.; Mackman, R. A. Development of Serine Protease Inhibitors Displaying a Multi-centered Short (<2.3 Å) Hydrogen Bond Binding Mode: Inhibitors of Urokinase-Type Plasminogen Activator and Factor Xa. *J. Med. Chem.* **2001**, *44*, 2753–2771.
- (24) Spencer, J. R.; McGee, D.; Allen, D.; Katz, B. A.; Luong, C.; Sendzik, M.; Squires, N.; Mackman, R. A. 4-Aminoarylguanidine and 4-Aminobenzamidines Derivatives as Potent and Selective Urokinase-type Plasminogen Activator Inhibitors. *Bioorg. Med. Chem. Lett.* **2002**, *12*, 2023–2026.
- (25) Nienaber, V. L.; Davidson, D.; Edalji, R.; Girande, V. L.; Klinghofer, V.; Henkin, J.; Magdalenos, P.; Mantei, R.; Merrick, S.; Severin, J. M.; Smith, R. A.; Stewart, K.; Walter, K.; Wang, J.; Wendt, M.; Weitzberg, M.; Zhao, X.; Rockway, T. Structure-directed discovery of potent nonpeptidic inhibitors of human urokinase that access a novel binding subsite. *Structure* **2000**, *8*, 553–563.
- (26) Klinghofer, V.; Stewart, K.; McGonigal, T.; Smith, R.; Sarthy, A.; Nienaber, V.; Butler, C.; Dorwin, S.; Richardson, P.; Weitzberg, M.; Wendt, M.; Rockway, T.; Zhao, X.; Hulkower, K. I.; Giranda, V. L. Species Specificity of Amidine-Based Urokinase Inhibitors. *Biochemistry* **2001**, *40*, 9125–9131.

- (27) Campagna, F.; Carotti, A.; Casini, G. A Convenient Synthesis of Nitriles From Primary Amides Under Mild Conditions. *Tetrahedron Lett.* **1977**, *18*, 1813–1816.
- (28) Boere, R. T.; Oakley, R. T.; Reed, R. W. Preparation of *N,N,N*-tris(trimethylsilyl)amidines; a convenient route to unsubstituted amidines. *J. Orgmet. Chem.* **1987**, *331*, 161–167.
- (29) Roger, R.; Neilson, D. G. The Chemistry of Imidates. *Chem. Rev.* **1961**, *61*, 179–211.
- (30) Brederick, H.; Gompper, R.; Seiz, H. Umsetzung Des Thioformamids Mit Halogenverbindungen. *Chem. Ber.* **1957**, *90*, 1837–1843.
- (31) Testaferri, L.; Tiecco, M.; Tingoli, M.; Chianelli, D.; Montanucci, M. Simple Syntheses of Aryl Alkyl Thioethers and of Aromatic Thiols from Unactivated Aryl Halides and Efficient Methods for Selective Dealkylation of Aryl Alkyl Ethers and Thioethers. *Synthesis* **1983**, 751–755.
- (32) Gray, N. M.; Cheng, B. K.; Mick, S. J.; Lair, C. M.; Contreras, P. C. Phencyclidine-like Effects of Tetrahydroisoquinolines and Related Compounds. *J. Med. Chem.* **1989**, *32*, 1242–1248.
- (33) Larsen, R. D.; Reamer, R. A.; Corley, E. G.; Davis, P.; Grabowski, E. J. J.; Reider, P. J.; Shinkai, I. A Modified Bischler-Napieralski Procedure for the Synthesis of 3-Aryl-3,4-dihydroisoquinolines. *J. Org. Chem.* **1991**, *56*, 6034–6038.
- (34) Quallich, G. J.; Makowski, T. W.; Sanders, A. F.; Urban, F. J.; Vazquez, E. Synthesis of 1,2,3,4-Tetrahydroisoquinolines Containing Electron-Withdrawing Groups. *J. Org. Chem.* **1998**, *63*, 4116–4119.
- (35) Park, K. K.; Oh, C. H.; Joung, W. K. Sodium Dithionite Reduction of Nitroarenes Using Viologen as an Electron Phase-Transfer Catalyst. *Tetrahedron Lett.* **1993**, *34*, 7445–7446.
- (36) Lemaire-Audoire, S.; Savignac, M.; Genet, J. P. Selective Deprotection of Allylamines using Palladium. *Tetrahedron Lett.* **1995**, *36*, 1267–1270.
- (37) (a) Maignan, S.; Mikol, V. The Use of 3D Structural Data in the Design of Specific Factor Xa Inhibitors. *Curr. Top. Med. Chem.* **2001**, *1*, 161–174. (b) Rai, R.; Sprengeler, P. A.; Elrod, K. C.; Young, W. B. Perspectives on Factor Xa Inhibition. *Curr. Med. Chem.* **2001**, *8*, 101–119. (c) Coburn, C. A. Small-molecule Direct Thrombin Inhibitors: 1997–2000. *Expert. Opin. Ther. Pat.* **2001**, *11*, 721–738. (d) Sanderson, P. E. J. Anticoagulants: Inhibitors of Thrombin and Factor Xa. *Ann. Rep. Med. Chem.* **2001**, *36*, 79–88.
- (38) Spraggon, G.; Phillips, C.; Nowak, U. K.; Ponting, C. P.; Saunders, D.; Dobson, C. M.; Stuart, D. I.; Jones, E. Y. The crystal structure of the catalytic domain of human urokinase-type plasminogen activator. *Structure* **1995**, *3*, 681–691.
- (39) Renatus, M.; Bode, W.; Huber, R.; Stürzebecher, J.; Stubbs, M. T. Structural and Functional Analyses of Benzamidine-Based Inhibitors in Complex with Trypsin: Implications for the Inhibition of Factor Xa, tPA, and Urokinase. *J. Med. Chem.* **1998**, *41*, 5445–5456.
- (40) (a) Katz, B. A.; Mackman, R.; Luong, C.; Radika, K.; Martelli, A.; Sprengeler, P. A.; Wang, J.; Chan, H.; Wong, L. Structural basis for selectivity of a small molecule, S1-binding, submicromolar inhibitor of urokinase-type plasminogen activator. *Chem. Biol.* **2000**, *7*, 299–312. (b) Katz, B. A.; Sprengeler, P. A.; Luong, C.; Verner, E.; Elrod, K.; Kirtley, M.; Janc, J.; Spencer, J. R.; Breitenbucher, J. G.; Hui, H.; McGee, D.; Allen, D.; Martelli, A.; Mackman, R. L. Engineering inhibitors highly selective for the S1 sites of Ser190 trypsin-like serine protease drug targets. *Chem. Biol.* **2001**, *8*, 1107–1121.
- (41) Wendt, M. D., unpublished results.
- (42) Dunitz, J. D. The Entropic Cost of Bound Water in Crystals and Biomolecules. *Science* **1994**, *264*, 670.
- (43) Nienaber, V.; Wang, J.; Davidson, D.; Henkin, J. Reengineering of human urokinase provides a system for structure-based drug design at high resolution and reveals a novel binding subsite. *J. Biol. Chem.* **2000**, *275*, 7239–7248.

JM0300072